European Journal of Medical Genetics 62 (2019) 224–228

Contents lists available at ScienceDirect

European Journal of Medical Genetics

journal homepage: www.elsevier.com/locate/ejmg

Two siblings with 11qter deletion syndrome that had been rescued in their mother by uniparental disomy

Miki Kawai[a], Makiko Tsutsumi[a], Fumihiko Suzuki[a,b], Kiyoko Sameshima[c], Yuri Dowa[d], Takuji Kyoya[e], Hidehito Inagaki[a,f], Hiroki Kurahashi[a,b,f,*]

[a] Division of Molecular Genetics, Institute for Comprehensive Medical Science, Fujita Health University, Toyoake, Japan
[b] Center for Collaboration in Research and Education, Fujita Health University, Toyoake, Japan
[c] Department of Pediatrics, Minamikyushu National Hospital, Aira, Japan
[d] Department of Neurology, Gunma Children's Medical Center, Shibukawa, Japan
[e] Department of Obstetrics, Gunma Children's Medical Center, Shibukawa, Japan
[f] Genome and Transcriptome Analysis Center, Fujita Health University, Toyoake, Japan

ARTICLE INFO

Keywords:
11q23-qter deletion
Jacobsen syndrome
Deletion rescue
Uniparental disomy
Skewed X chromosome inactivation
Germline mosaicism

ABSTRACT

Jacobsen syndrome refers to a congenital anomaly caused by deletion at 11q23.3-qter. We here describe two siblings with the same 11q23.3-qter deletion. Both parents were healthy with a normal karyotype. Cytogenetic microarray analysis revealed no mosaicism in either parent but the mother showed uniparental disomy encompassing the deleted region found in the two siblings. The pattern of X chromosome inactivation was almost completely skewed in the mother. These data suggested that the mother was a carrier of the 11q23.3-qter deletion but that this had been rescued by disomy formation during early embryogenesis except for her germinal cells.

1. Introduction

Jacobsen syndrome (MIM#147791) is a contiguous gene deletion syndrome caused by deletion of the 11qter region. The typical clinical features of Jacobsen syndrome include pre- and postnatal physical growth and psychomotor retardation, facial dysmorphic features, and thrombocytopenia. Some patients with this syndrome also have malformations of the heart, kidney, gastrointestinal tract, and central nervous system. Ocular and hearing problems can be also present. The estimated occurrence of Jacobsen syndrome is about 1/100,000 births (Mattina et al., 2009).

About 85% of Jacobsen syndrome cases are caused by a simple *de novo* terminal deletion. Other cases result from a variety of chromosomal abnormalities including segregation of a familial reciprocal balanced translocation, *de novo* unbalanced translocations, recombination of a parental pericentric inversion, or other rearrangements such as ring chromosomes. An 11q deletion has also been reported in the mosaic form of this condition. The breakpoints in these deletions occur within or distal to 11q23.3, and the deletions usually extend to the telomere (Grossfeld et al., 2004). The deletion size ranges from 7 to 20 Mb. The chromosomal region conferring specificity for the Jacobsen syndrome phenotype is the 11q24.2 band, but the gene responsible for this phenotype is still unknown.

We here report on two siblings with the same 11q23.3-qter deletion, one with Jacobsen syndrome and the other detected by amniocentesis and terminated. The parents however showed a normal karyotype. Cytogenetic microarray analyses revealed that the healthy mother had uniparental disomy (UPD) encompassing the 11q22.3-ter region deleted in the siblings. A possible mechanism for the recurrence of this deletion is discussed.

2. Clinical report

A 4-year old Japanese male subject was the first child of a non-consanguineous healthy 36-year old father and 28-year old mother after having three miscarriages with no notable family history of disease (Fig. 1A). At 22 weeks of pregnancy, a congenital heart defect, mitral valve stenosis and aortic valve stenosis were suspected. He had been born after a 41 week gestation by an induced labor with a birth weight of 2644 g (−0.9SD), height of 47.5 cm (−0.7SD), head circumference of 34.5 cm (+0.8SD), and chest circumference of 30 cm. He showed a hypoplastic left heart, conductive auditory impairment in the left ear,

* Corresponding author. Division of Molecular Genetics, Institute for Comprehensive Medical Science, Fujita Health University, 1-98 Dengakugakubo, Kutsukake-cho, Toyoake, Aichi, 470-1192, Japan.
E-mail address: kura@fujita-hu.ac.jp (H. Kurahashi).

https://doi.org/10.1016/j.ejmg.2018.07.018
Received 1 March 2018; Received in revised form 12 June 2018; Accepted 17 July 2018
Available online 18 July 2018
1769-7212/

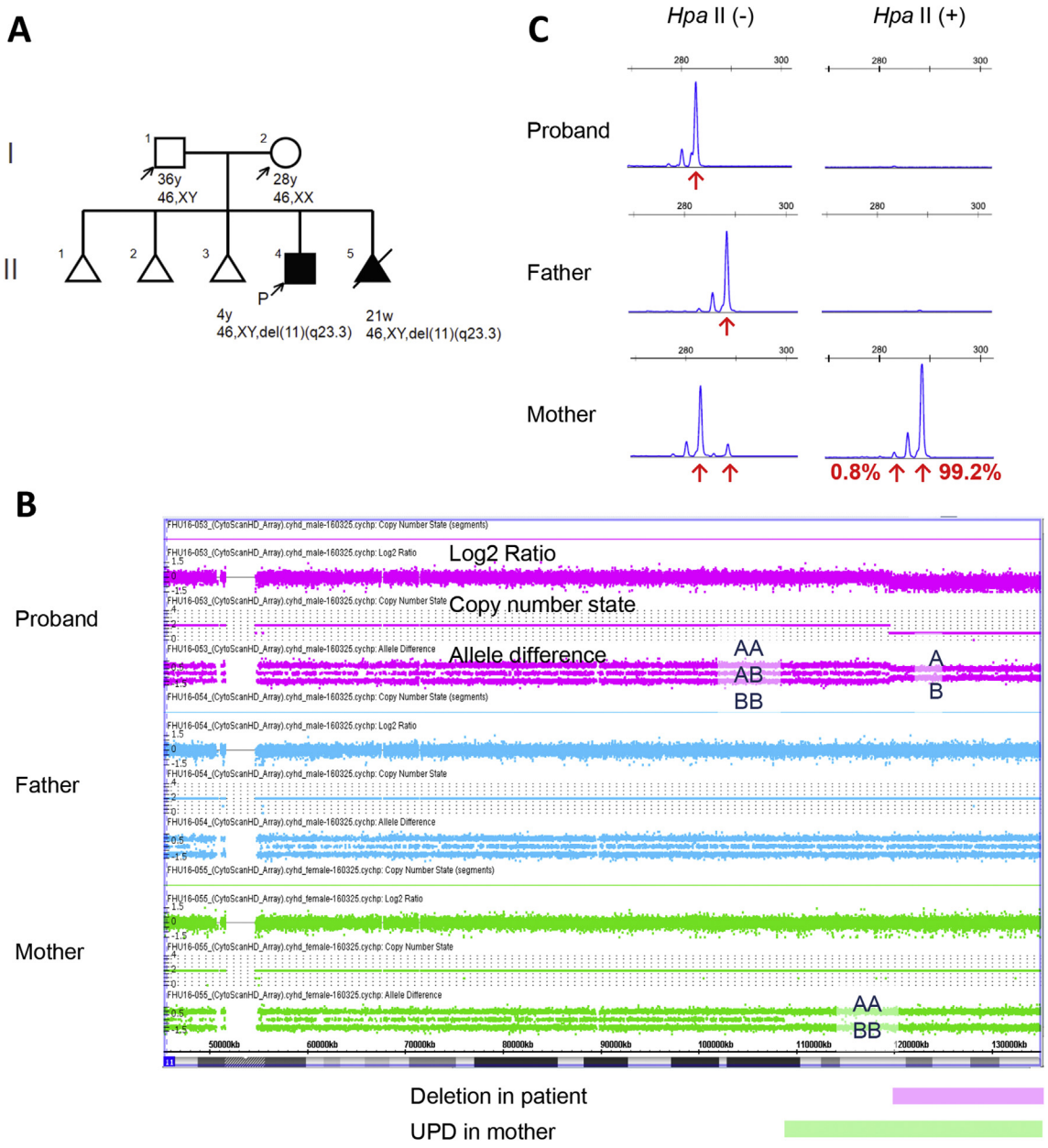

Fig. 1. Deletion rescue on 11qter. **(A)** Pedigree of the study family. **(B)** Cytogenetic microarray results for the 11q region for the proband (pink), father (blue), and mother (green). The copy number log2 ratio (top), copy number state (middle), and allele difference (bottom) are shown for each sample. The pink bar at the bottom indicates the deleted region in the proband. The green bar indicates the UPD region in the mother. **(C)** HUMARA assay results. The electropherogram shows the fragment analysis of the amplicons from undigested (left) and digested (right) genomic DNA from the proband (top), father (middle), and mother (bottom). The major peaks depicted by the red arrows indicate the sizes of the PCR products with different numbers of short tandem repeats at the HUMARA locus. The two major peaks found in the mother represent two X chromosome alleles (282bp, 288bp). Digestion of the DNA from the proband (son)'s and father's sample showed complete loss of one allele, whereas a preferential loss of the short alleles was evident in the mother (282bp). (For interpretation of the references to colour in this figure legend, the reader is referred to the Web version of this article.)

widely spaced eyes, a short nose, a small ear lobe, thin vermilion of upper lip and lower lip, shortness in both fifth fingers, and a bifid scrotum. He also had an old cerebral hemorrhage in the nucleus basalis.

The subject also showed severely retarded psychomotor development. The ability to hold up his head, roll over, and speak, were recognized at 2 years and 7 months, 2 years and 7 months, and 3 years and 3 months. Serial complete blood counts revealed transient thrombocytopenia. At the age of 4 years and 2 months, he showed a height of −3.5SD, weight of −2.2SD, and head circumference of −1.2SD. His karyotype revealed 46,XY,del (11) (q23.3), which is known as Jacobsen syndrome.

At 2 years after the birth of this first child, the mother again became pregnant with a boy. The fetus was diagnosed with the same karyotype as the brother by amniocentesis at 15 weeks and 4 days of gestation. At 20 weeks and 4 days, a hypoplastic left heart with severe atrioventricular regulation was evident on ultrasound examination. At 21 weeks, the pregnancy was terminated and the fetus was found to weigh 344 g. Karyotype analysis of the parental peripheral blood lymphocytes revealed 46, XY [20] and 46, XX [20].

3. Materials and methods

3.1. Subjects

Peripheral blood samples were obtained from the study subject and the parents. The research protocol for this study was approved by the local ethics committee of Fujita Health University, Japan. Written informed consent to participate in the study was obtained from the parents.

3.2. DNA extraction

Genomic DNA was extracted from whole blood using QuickGene 610 L (Fuji film, Tokyo, Japan). The concentration of the DNA was measured using an ND-1000 spectrophotometer (NanoDrop, Wilmington, DE) and the quality was determined by gel electrophoresis.

3.3. Cytogenetic microarray

High-resolution chromosomal microarray analysis using the CytoScan HD array (Affymetrix, Santa Clara, CA) was performed. DNA samples of 50 ng were used in this analysis in accordance with the manufacturer's instructions. The genomic coordinates were based upon genome build 37/hg19 (2009). Hybridization, data extraction and analysis were performed as per the manufacturer's protocols. Chromosome Analysis Suite software 3.0 (ChAS, Affymetrix Santa Clara, CA) was used for raw data analysis, review and reporting. Regions of copy-number changes were extracted with 20 probes of 50 kb. All of the extracted regions containing a copy-number change were confirmed by visual comparisons with the normal control data from Database of Genomic Variants (http://dgv.tcag.ca). UPD regions were extracted with 5 Mb. Regions with a sparse SNP density were carefully evaluated to exclude false calls.

3.4. FISH analysis

Peripheral blood lymphocytes and buccal samples were obtained by standard methods. FISH analysis was performed using standard techniques. The probes used for the FISH analysis were TelVysion 11p SpectrumGreen (D11S2071), TelVysion 11q SpectrumOrange (D11S1037) (Abbott Molecular, IL, USA). A hundred interphases nuclei were analyzed for pter/qter of chromosome 11.

3.5. HUMARA assay

To assess skewing of the X chromosome inactivation, we performed HUMARA assay according to the protocol described elsewhere (Beever et al., 2003). Briefly, we digested the genomic DNA with methylation-sensitive restriction enzyme *Hpa*II. PCR primers, one of which was labeled with FAM, were designed across the polymorphic CAG repeat as well as two *Hpa*II sites in the androgen receptor gene on the X chromosome. PCR amplification would be achieved only from the inactivated allele having the *Hpa*II sites methylated. PCR products were analyzed by capillary electrophoresis (ABI3730 Genetic Analyzer) and quantified the area under the curve using GeneMapper software.

4. Results

We performed cytogenetic microarray analysis to demarcate the deleted region in our current case subject. A 15.4-Mb region was found to have been deleted at 11q23.3q25-qter in this patient (arr [hg19] 11q23.3q25 (119, 484, 933_134, 938, 470) × 1), which is consistent with the typically deleted region in Jacobsen syndrome (Fig. 1B). The deleted region was found to contain 128 Refseq genes, and 70 OMIM genes. Single nucleotide polymorphism (SNP) genotyping indicated that the deleted chromosome was derived from the mother (data not shown).

A possible explanation for the abnormal 46,XY,del (11) (q23.3) karyotype in two siblings from parents with a normal karyotype was that one of the parents harbored FRA11B, a (CCG)n repeat expansion in the 5′untranslated region of the *CBL2* gene. In more than 70% of normal individuals, this repeat is present in 11 copies but can be expanded to several hundred copies and lead to genomic instability and a susceptibility for terminal deletion (Mattina et al., 2009). However, the deletion breakpoint of our current patient was at chr11:119, 484, 933 (hg19), which is approximately 400 kb distal from FRA11B.

Neither of the parents showed deletion mosaicism at the 11q23.3-qter region. Interphase FISH on 100 peripheral blood lymphocytes and 100 buccal cells revealed no deletion for the 11q subtelomere-specific probe (data not shown). It was notable however that SNP array analysis of the patient's mother detected a 26.2-Mb region with a loss of heterozygosity at 11q22.3-qter consistent with uniparental disomy (UPD) (arr [hg19]11q22.3q25 (108, 657, 506_134, 942, 626) × 2 hmz) (Fig. 1B). The deletion breakpoint in the son was 10-Mb distal from the UPD boundary in the mother.

A HUMARA assay was performed to determine when the UPD was generated in the mother. The patterns of X chromosome inactivation (XCI) showed 99.2% skewing in the mother (Fig. 1C), suggesting that she originally had the same deletion as her son and the chromosome copy number loss was corrected by UPD after XCI occurred in the early embryogenesis.

5. Discussion

Our analysis by cytogenetic microarray of our current case subject with 11qter deletion syndrome and his family suggests that segmental UPD corrected the chromosomal copy number of the deleted region and thereby rescued the phenotype in his healthy mother. To our knowledge, there have only been two previous reports of siblings showing a deletion of 11q23.3-qter despite a normal parental karyotype (Afifi et al., 2008; Johnson et al., 2014). One of those reports also provided detailed molecular analyses showing a maternal UPD at the 11qter region (Johnson et al., 2014). A 22q13 deletion rescued by paternal UPD has also been reported (Bonaglia et al., 2009). Such deletion rescue event has not been reported for other terminal deletions. Our current case is therefore the third report to describe a deletion rescued by post-zygotic UPD generation.

It is likely that the mother of our current case subject originally carried the 11q23-qter deletion that had been transmitted from a gamete of a maternal grandfather or grandmother. After fertilization, this deletion was likely rescued during the post-zygotic stage via a DNA repair pathway for coincidental double-strand-breaks (DSBs) at the proximal region of the deletion breakpoint, thereby generating the segmental UPD. The UPD boundary in the mother is located 10 Mb more proximal than the breakpoint of deleted region of the patient, which is a strong evidence that the UPD developed after the deletion. The principal molecular mechanisms that have been postulated to explain segmental UPD are mitotic recombination or break-induced replication (BIR) (Costantino et al., 2014; Carvalho et al., 2015).

We observed an almost completely skewed XCI in the mother's DNA. Generally, an XCI pattern increases the extent of skewing with age as a consequence of hematopoietic stem cell senescence. At 20–39 years old, mean skewing level is reported to be 70.6% (Hatakeyama et al., 2004). Our current patient's mother was 30 years old at the time of genetic testing and showed very high skewing at 99.2%. This indicated that her blood cells were derived from a single clone after XCI (Kurahashi et al., 1991). We speculated that the mother originally harbored the 11q23-qter deletion as a zygote which was subsequently repaired in one of the somatic cells by mitotic recombination or BIR after XCI has been completed. The repaired cell likely obtained selective advantage during embryonic development and unrepaired cells were eliminated (Fig. 2). This resulted in a normal phenotype at birth and no evidence of

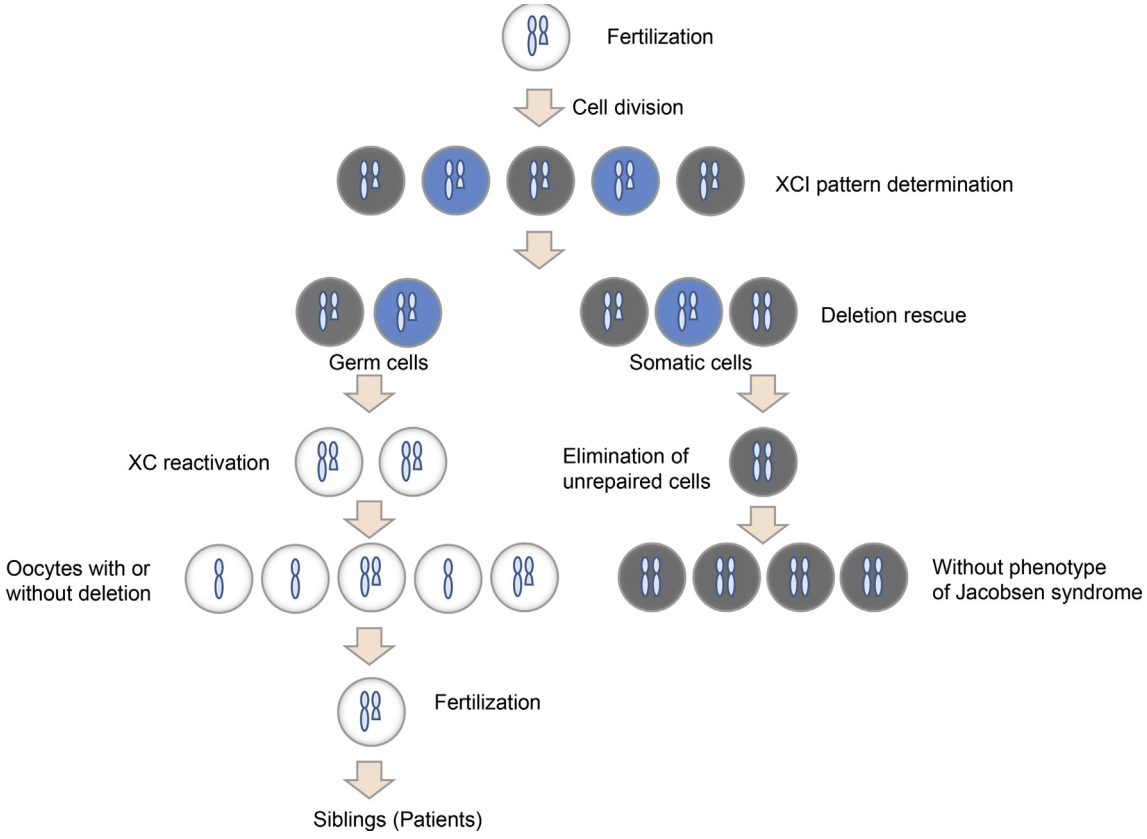

Fig. 2. An illustration for the status of the mother and the two siblings.

Jacobsen syndrome. It appears however that although her somatic cells had all been rescued by UPD her germ cells retained the 11q23-qter deletion. Such monoclonality has been described previously in trisomy rescue of chromosome 15 (Butler et al., 2007). Thus, this mother had no Jacobsen syndrome phenotype but transmitted the causative deletion to her two sons.

As far as we are aware, there have been only two other case reports of 'deletion rescue' (Bonaglia et al., 2009; Johnson et al., 2014). It would be intriguing if 11q23.3-qter was found to be a hotspot for deletion rescue. One possible explanation for this phenomenon is a strong negative selection process as a result of gene loss. An alternative possibility is that there might be a DSB hotspot that induces mitotic recombination or BIR at the region proximal to the 11q23.3 breakpoint. If this is indeed the case, the recurrence risk in the affected siblings would be slightly higher than in the general population. SNP array analysis of the parents might be advisable even in an apparent *de novo* case of Jacobsen syndrome.

In conclusion, we speculate that the maternal 11q23.3-qter deletion was repaired in our current study family via mitotic recombination or BIR leading to UPD generation. As a consequence of this DNA repair, the chromosomal copy number was corrected in the mother resulting in a normal phenotype. On the other hand, some of maternal germline cells retained 11q23-ter deletion, leading to a recurrence of Jacobsen syndrome in her offspring. Careful genetic counseling is therefore warranted regarding the recurrence of Jacobsen syndrome.

Acknowledgements

We thank the parents of our patient subject for agreeing to participate in this study. We also thank Naoko Fujita and Asami Kuno for technical assistance. This study was supported by grants-in-aid for Scientific Research from the Ministry of Education, Culture, Sports, Science and Technology of Japan (15H04710), from the Ministry of Health, Welfare and Labor (H27-Nanchitou-Ippan(nan)-024), and from the Japan Agency for Medical Research and Development (17ek0109151h0003).

References

Afifi, H.H., Zaki, M.S., El-Gerzawy, A.M., Kayed, H.F., 2008. Distal 11q monosomy syndrome: a report of two Egyptian sibs with normal parental karyotypes confirmed by molecular cytogenetics. Genet. Counsel. 19, 47–58.

Beever, C.L., Stephenson, M.D., Peñaherrera, M.S., Jiang, R.H., Kalousek, D.K., Hayden, M., Field, L., Brown, C.J., Robinson, W.P., 2003. Skewed x-chromosome inactivation is associated with trisomy in women ascertained on the basis of recurrent spontaneous abortion or chromosomally abnormal pregnancies. Am. J. Hum. Genet. 72, 399–407. https://doi.org/10.1086/346119.

Bonaglia, M.C., Giorda, R., Beri, S., Bigoni, S., Sensi, A., Baroncini, A., Capucci, A., De Agostini, C., Gwilliam, R., Deloukas, P., Dunham, I., Zuffardi, O., 2009. Mosaic 22q13 deletions: evidence for concurrent mosaic segmental isodisomy and gene conversion. Eur. J. Hum. Genet. 17, 426–433. https://doi.org/10.1038/ejhg.2008.195.

Butler, M.G., Theodoro, M.F., Bittel, D.C., Kuipers, P.J., Driscoll, D.J., Talebizadeh, Z., 2007. X-chromosome inactivation patterns in females with Prader–Willi syndrome. Am. J. Med. Genet. 143A, 469–475.

Carvalho, C.M.B., Pfundt, R., King, D.A., Lindsay, S.J., Zuccherato, L.W., Macville, M.V.E., Liu, P., Johnson, D., Stankiewicz, P., Brown, C.W., Shaw, C.A., Hurles, M.E., Ira, G., Hastings, P.J., Brunner, H.G., Lupski, J.R., 2015. Absence of heterozygosity due to template switching during replicative rearrangements. Am. J. Hum. Genet. 96, 555–564. https://doi.org/10.1016/j.ajhg.2015.01.021.

Costantino, L., Sotiriou, S.K., Rantala, J.K., Magin, S., Mladenov, E., Helleday, T., Haber, J.E., Iliakis, G., Kallioniemi, O.P., Halazonetis, T.D., 2014. Break-induced replication repair of damaged forks induces genomic duplications in human cells. Science 343 (80), 88–91. https://doi.org/10.1126/science.1243211.

Grossfeld, P.D., Mattina, T., Lai, Z., Favier, R., Jones, K.L., Cotter, F., Jones, C., 2004. The 11q terminal deletion disorder: a prospective study of 110 cases. Am. J. Med. Genet. 129A, 51–61. https://doi.org/10.1002/ajmg.a.30090.

Hatakeyama, C., Anderson, C.L., Beever, C.L., Peñaherrera, M.S., Brown, C.J., Robinson, W.P., 2004. The dynamics of X-inactivation skewing as women age. Clin. Genet. 66, 327–332. https://doi.org/10.1111/j.1399-0004.2004.00310.x.

Johnson, J.P., Haag, M., Beischel, L., Mccann, C., Phillips, S., Tunby, M., Hansen, J., Schwanke, C., Reynolds, J.F., 2014. "Deletion rescue" by mitotic 11q uniparental disomy in a family with recurrence of 11q deletion Jacobsen syndrome. Clin. Genet. 85, 376–380. https://doi.org/10.1111/cge.12164.

Kurahashi, H., Hara, J., Yumura-Yagi, K., Murayama, N., Inoue, M., Ishihara, S., Tawa, A.,

Okada, S., Kawa-Ha, K., 1991. Monoclonal nature of transient abnormal myelopoiesis in Down's syndrome. Blood 77, 1161–1163.
Mattina, T., Perrotta, C.S., Grossfeld, P., 2009. Jacobsen syndrome. Orphanet J. Rare Dis. 4, 1–10. https://doi.org/10.1186/1750-1172-4-9.

International Journal of Cardiology 274 (2019) 290–295

Contents lists available at ScienceDirect

International Journal of Cardiology

journal homepage: www.elsevier.com/locate/ijcard

Frequent intragenic microdeletions of elastin in familial supravalvular aortic stenosis

Satoshi Hayano [a,1], Yusuke Okuno [b,1], Makiko Tsutsumi [c,1], Hidehito Inagaki [c,1], Yoshie Fukasawa [a,1], Hiroki Kurahashi [c,1], Seiji Kojima [a,1], Yoshiyuki Takahashi [a,1], Taichi Kato [a,*,1]

[a] Department of Pediatrics, Nagoya University Graduate School of Medicine, 65 Tsurumai-cho, Showa-ku, Nagoya, Japan
[b] Center for Advanced Medicine and Clinical Research, Nagoya University Hospital, 65 Tsurumai-cho, Showa-ku, Nagoya, Japan
[c] Division of Molecular Genetics, Institute for Comprehensive Medical Science, Fujita Health University, 1-98 Dengakugakubo, Kutsukake-cho, Toyoake, Japan

ARTICLE INFO

Article history:
Received 10 April 2018
Received in revised form 1 September 2018
Accepted 7 September 2018
Available online 13 September 2018

Keywords:
Supravalvular aortic stenosis
Elastin
Congenital heart defects
Whole exome sequencing

ABSTRACT

Background: Supravalvular aortic stenosis (SVAS) is a congenital heart disease affecting approximately 1:25,000 live births. SVAS may occur sporadically, be inherited in an autosomal dominant manner, or be associated with Williams-Beuren syndrome, a complex developmental disorder caused by a microdeletion of chromosome 7q11.23. *ELN* on 7q11.23, which encodes elastin, is the only known gene to be recurrently mutated in less than half of SVAS patients.
Methods: Whole-exome sequencing (WES) was performed for seven familial SVAS families to identify other causative gene mutations of SVAS.
Results: Three truncating mutations and three intragenic deletions affecting *ELN* were identified, yielding a diagnostic efficiency of 6/7 (85%). The deletions, which explained 3/7 of the present cohort, spanned 1–29 exons, which might be missed in the course of mutational analysis targeting point mutations. The presence of such deletions was validated by both WES-based copy number estimation and multiplex ligation-dependent probe amplification analyses, and their pathogenicity was reinforced by co-segregation with clinical presentations.
Conclusions: The majority of familial SVAS patients appear to carry *ELN* mutations, which strongly indicates that elastin is the most important causative gene for SVAS. The frequency of intragenic deletions highlights the need for quantitative tests to analyze *ELN* for efficient genetic diagnosis of SVAS.

1. Introduction

Supravalvular aortic stenosis (SVAS; MIM #185500) is a congenital heart disease affecting approximately 1:25,000 live births [1]. Congenital narrowing of the lumen of the ascending aorta or peripheral pulmonary arteries provokes increased resistance to blood flow and causes elevated ventricular pressure and hypertrophy resulting in heart failure. Peripheral pulmonary stenosis (PPS) is known to occasionally coexist with SVAS [2]. Approximately 30% to 50% of patients with SVAS have Williams-Beuren Syndrome (WBS; MIM #194050) [2–4], which is a complex genetic disorder caused by 7q11.23 microdeletion and characterized by growth failure, a characteristic facial appearance (so-called "Elfin face"), mental retardation, and SVAS [5].

On the other hand, Eisenberg et al. first reported non-syndromic "familial SVAS" with autosomal dominant inheritance in 1964 [3], accounting for 20% of SVAS cases (approximately 1:125,000 live births) [6]. These patients showed normal intelligence and lacked the dysmorphic features of WBS. Genetic analysis including linkage analysis identified *ELN*, which encodes elastin, as a causative gene of non-syndromic familial SVAS [1,7–17]. In harmony with the genetic findings, luminal obstruction of the aorta was shown in a transgenic mouse model carrying homozygous or heterozygous elastin gene deletion [18,19].

Metcalfe et al. sequenced *ELN* exons of patients with non-syndromic SVAS, which showed truncating mutations in 35 cases, but no causative variants were found in the remaining 64 patients (of which 8 were familial cases) [20]. Micale et al. also investigated *ELN* gene mutations in 14 familial and 10 sporadic cases of SVAS, resulting in 7 novel mutations, including 5 frameshift and 2 donor splice site mutations, but found no *ELN* gene abnormality in the remaining 17 cases [21]. Therefore, less than half of the cases could be explained by *ELN* mutations, whereas it still remains unclear whether *ELN* could explain the remaining cases

* Corresponding author.
E-mail addresses: javauma@gmail.com (S. Hayano), yusukeokuno@gmail.com (Y. Okuno), makiko@fujita-hu.ac.jp (M. Tsutsumi), hinagaki@fujita-hu.ac.jp (H. Inagaki), love.rodin.love@gmail.com (Y. Fukasawa), kura@fujita-hu.ac.jp (H. Kurahashi), kojimas@med.nagoya-u.ac.jp (S. Kojima), ytakaha@med.nagoya-u.ac.jp (Y. Takahashi), ktaichi@med.nagoya-u.ac.jp (T. Kato).
[1] This author takes responsibility for all aspects of the reliability and freedom from bias of the data presented and their discussed interpretation.

https://doi.org/10.1016/j.ijcard.2018.09.032
0167-5273/

Abbreviations

SVAS	supravalvular aortic stenosis
WES	whole-exome sequencing
PPS	peripheral pulmonary stenosis
WBS	Williams-Beuren syndrome
FISH	fluorescence in situ hybridization
MLPA	Multiplex ligation-dependent probe amplification

with SVAS, or there are unidentified causative genes. In this study, whole-exome sequencing (WES) was performed with careful assessment of *ELN* mutations, including copy number analysis, to elucidate the genetic background of SVAS.

2. Methods

2.1. Sample collection

This study included seven families of Japanese ancestry with autosomal dominant inheritance of SVAS. There was no developmental delay or dysmorphic features suggestive of WBS or positive fluorescence in situ hybridization (FISH) on 7q11.23 in any family members. The vascular malformation (SVAS and PPS) was diagnosed if the sinotubular junction of the aorta was smaller than the diameter of the aortic annulus and significant pressure gradients were measurable by echocardiogram and/or angiographically [6]. Written, informed consent was obtained from patients or their parents, and whole blood or saliva was collected. Saliva samples were collected using an Oragene DNA self-collection kit (DNA Genotek, Ottawa, Canada). Genomic DNA was extracted from whole blood or saliva using the QIAamp DNA Blood Mini kit (Qiagen, Hilden, Germany), according to the manufacturer's instructions. The study was approved by the Ethics Committee of the Nagoya University Graduate School of Medicine (approval number 2015–0032).

2.2. Whole-exome sequencing analysis

Exome capture was performed on each proband using SureSelect Human All Exon V5 (Agilent Technologies, Santa Clara, CA), according to the manufacturer's instructions. Generated libraries were sequenced on a HiSeq 2500 platform (Illumina, San Diego, CA). Sequence data were analyzed using an in-house pipeline [22]. Briefly, reads were aligned to UCSC build hg19 reference genome using the Burrows-Wheeler Aligner [23]. Picard tools (http://broadinstitute.github.io/picard) were utilized to remove PCR duplicates. Variants were called using VarScan2, where a variant allele frequency of >0.20 was used as a cutoff [24]. ANNOVAR was used together with in-house scripts to annotate genetic variants [25]. The average depth of coverage across the whole exome for each sample achieved was 111.14 (range 90.68 to 127.66), and the number of mutations found per sample ranged from 25,534 to 25,920.

2.3. Mutational analysis

Mutational analysis to define each variant's pathogenicity was essentially based on the latest release of the American College of Medical Genetics (ACMG) guideline [26]. Briefly, variants outside of coding regions and common variants with >1% minor allele frequency in the National Heart, Lung, and Blood Institute ESP (Exome Sequencing Project) 6500 [27], 1000 Genomes Project [28], ExAC (Exome Aggregation Consortium) [29], HGVD (Human Genetic Variation Database) [30], or the in-house database were excluded. Variants expected to cause the disorders (eg, missense variants with reported pathogenicity and nonsense, frameshift insertion/deletion, and splice-site variants on genes known to cause a disease by inactivation) were validated by Sanger sequencing using PrimeSTAR GXL DNA polymerase (Takara, Shiga, Japan) and the Big Dye Terminator 3.1 Cycle Sequencing Kit (Thermo Fisher Scientific Inc., Waltham, MA) with ABI PRISM 3130xL (Applied Biosystems, Foster City, CA). Primer sequences are listed in Table S1.

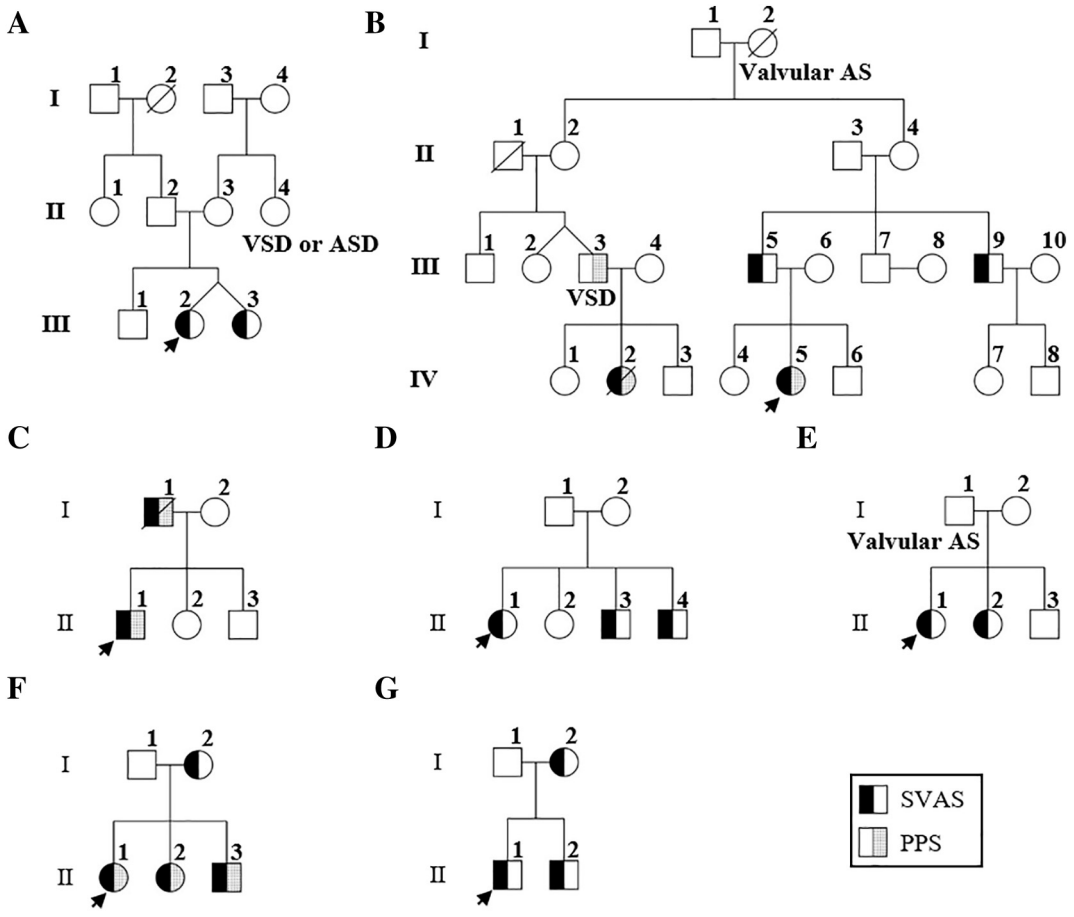

Fig. 1. Pedigree chart of families with familial supravalvular aortic stenosis Arrows indicate probands for whom whole-exome sequencing was performed. SVAS, supravalvular aortic stenosis; PPS, peripheral pulmonary stenosis; VSD, ventricular septal defect; ASD, atrial septal defect; AS, aortic stenosis.

2.4. Copy number analysis

Copy number analysis was performed by comparing the number of reads conveying each exon normalized by the mean depth of the entire sample with that of unrelated normal DNA samples, as we have previously shown [22]. Exons of normalized coverage >3 standard deviations (SDs) or less than −3 SDs from the mean coverage of reference samples were considered to be candidates for copy number variants. Multiplex ligation-dependent probe amplification (MLPA) according to the manufacturer's protocol with the SALSA MLPA P029-WBS probemix (MRC Holland, Amsterdam, Netherlands), which includes 10 exons of the *ELN* gene (Exon 1, 3, 4, 6, 9, 16, 20, 26, 27 and 33), was performed to validate candidate exonic deletions detected in the *ELN* gene by WES analysis. MLPA analysis software Coffalyser (MRC Holland) was used to identify CNVs.

3. Results

WES-based detection of point mutations and copy number alterations was performed in seven families of Japanese ancestry with SVAS showing an autosomal dominant mode of inheritance (Fig. 1). Three heterozygous pathogenic mutations in *ELN* (c.370delT, p.Ser124Leufs*13 in family A, c.572-1G > A splice site mutation affecting the acceptor of exon 12 in family B, and c.218_219insTG, p.Gly74Valfs*49 in family C) were identified. All of these mutations were novel, and they were validated on all available family members by Sanger sequencing (Fig. S1). Mutations were present

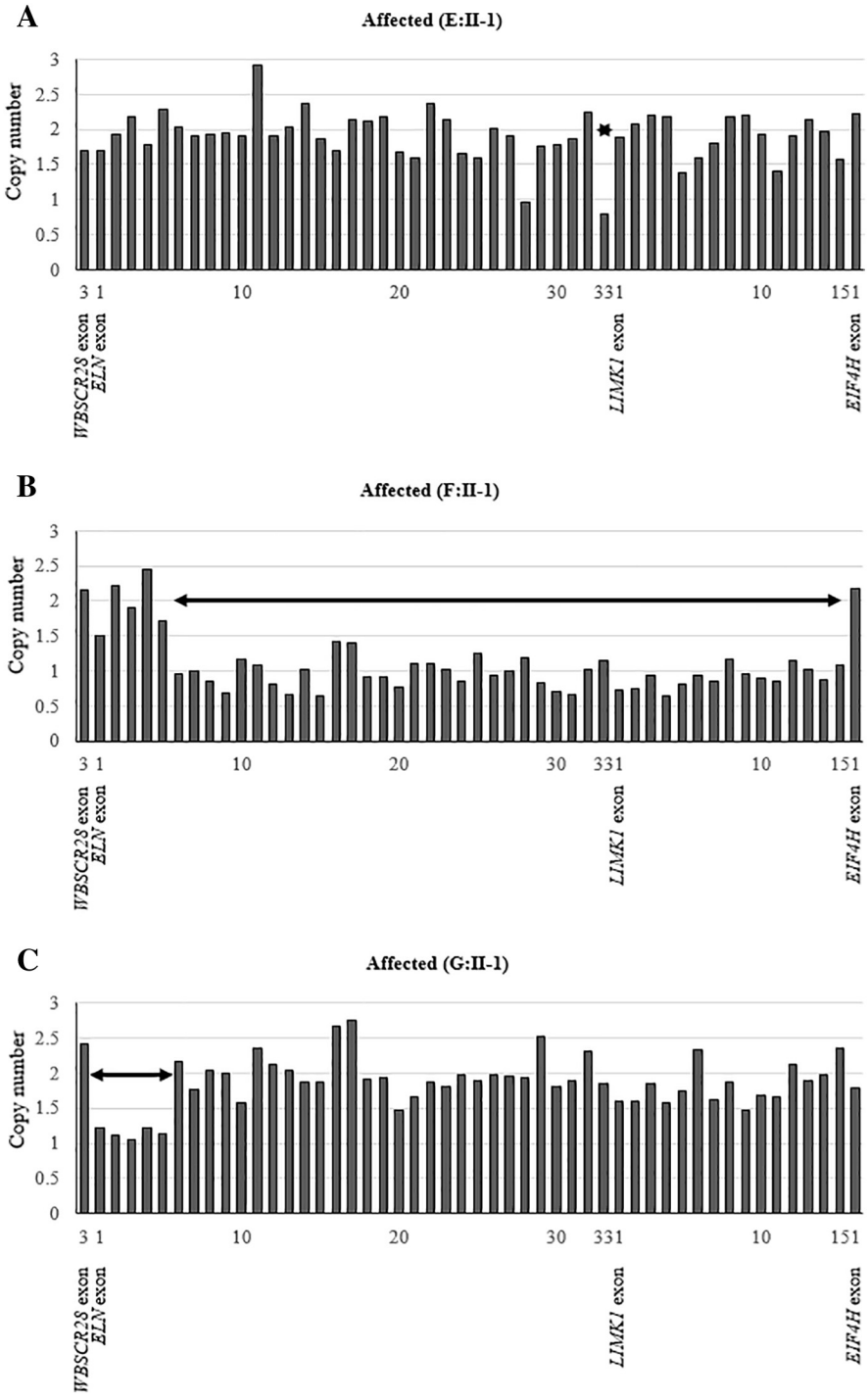

Fig. 2. Copy-number analysis The estimated copy number of each exon based on the number of reads in each exon in whole-exome sequencing. Each bar represents an exon, and the vertical axis represents the estimated copy number. Arrows indicate estimated deleted regions.

Table 1
Phenotype and segregation of *ELN* mutations.

Family	Subject	Phenotype	*ELN* mutation
A	II-2	–	–
	II-3	–	c.370delT, p.Ser124Leufs*13
	III-1	–	–
	III-2	SVAS	c.370delT, p.Ser124Leufs*13
	III-3	SVAS	c.370delT, p.Ser124Leufs*13
B	III-3	PPS, VSD	c.572-1G > A splice site
	III-5	SVAS	c.572-1G > A splice site
	III-6	–	–
	IV-4	–	–
	IV-5	SVAS, PPS	c.572-1G > A splice site
	IV-6	–	–
C	I-2	–	–
	II-1	SVAS, PPS	c.218_219insTG, p.Gly74Valfs*49
	II-2	–	–
	II-3	–	c.218_219insTG, p.Gly74Valfs*49
D	II-1	SVAS	–
E	I-1	Valvular AS	Microdeletion (exon 33)
	I-2	–	–
	II-1	SVAS	Microdeletion (exon 33)
	II-2	SVAS	Microdeletion (exon 33)
	II-3	–	–
F	I-1	–	–
	I-2	SVAS	Microdeletion (exon 5–33)
	II-1	SVAS, PPS	Microdeletion (exon 5–33)
	II-2	SVAS, PPS	Microdeletion (exon 5–33)
	II-3	SVAS, PPS	Microdeletion (exon 5–33)
G	I-1	–	–
	I-2	SVAS	Microdeletion (exon 1–5)
	II-1	SVAS	Microdeletion (exon 1–5)
	II-2	SVAS	Microdeletion (exon 1–5)

All mutations were heterozygous.
SVAS, supravalvular aortic stenosis; PPS, peripheral pulmonary stenosis; VSD, ventricular septal defect; AS, aortic stenosis.

in all patients and several family members without SVAS, indicating incomplete penetrance (Table 1).

Copy number aberrations in *ELN* were identified in three other families, all of which were deletions (exon 33 in family E, exons 5–33 in family F, and exons 1–5 in family G, Fig. 2). Such deletions were validated by MLPA (Fig. S2). All microdeletions showed complete co-segregation with clinical symptoms (Table 1).

In the remaining family D, no diagnostic mutations associated with SVAS could be identified in the proband (D:II-1) either by WES or MLPA (Table S2, Fig. S3).

4. Discussion

Pathogenic mutations or deletions in *ELN* gene were identified in six of seven families with autosomal dominant inheritance of SVAS, including three novel point mutations and three intragenic deletions. These findings suggest that intragenic deletions in *ELN* gene could explain the genetic cause in half of so-far unexplained cases with familial SVAS in Japan. Updated by these findings, a comprehensive list of reported pathogenic SVAS mutations is provided (Fig. 3) [7–9,12,17,20,21,31–38].

ELN encodes elastin, which is expressed in various tissues and organs, including smooth muscle cells of the great arteries, and contributes to tissue elasticity [39,40]. The molecular mechanism of the pathogenesis of SVAS is not fully elucidated. However, considering accumulating knowledge from patients and transgenic mice [18,19,21,41], it seems likely that mutations of *ELN* impair vascular elasticity, and increased shear stress in the vascular wall could result in SVAS [39,40].

The microdeletions of *ELN* gene shown in the present study were not identified with existing FISH probes for WBS. There are a few case reports showing that microdeletions of *ELN* gene are the cause of SVAS [8,9]. The present finding raises the necessity to investigate the

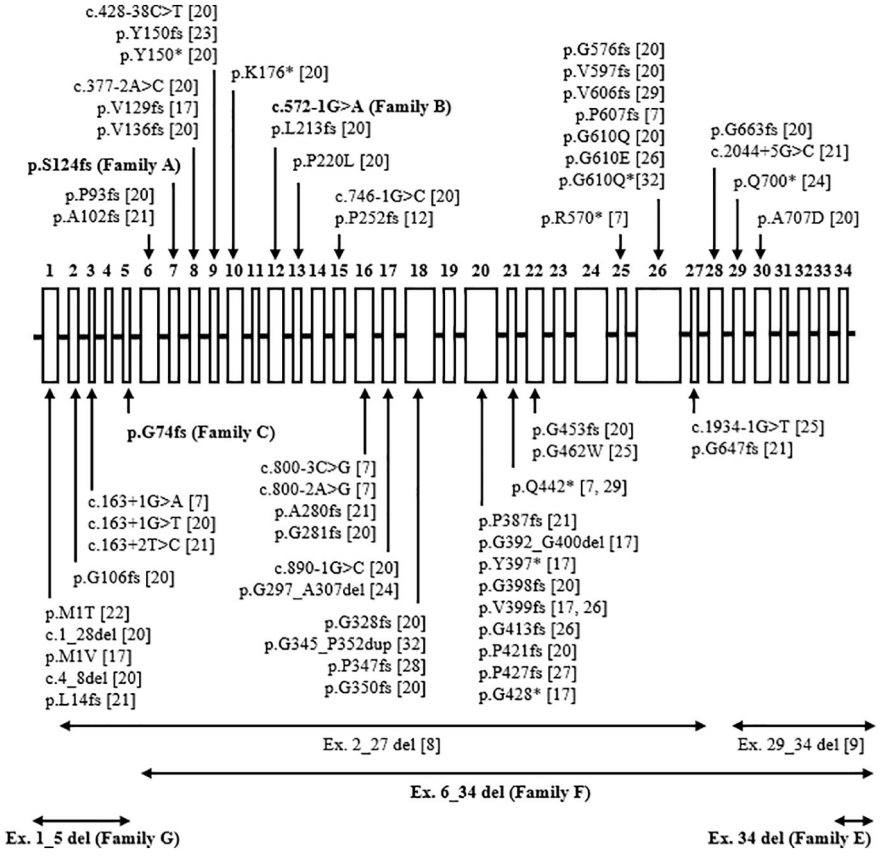

Fig. 3. *ELN* cDNA showing the exons and mutations detected This figure summarizes previously reported and newly identified mutations for familial and sporadic SVAS. The numbers above open boxes indicate the exon numbers. The present findings are shown in bold letters.

exon-spanning deletions affecting *ELN* using MLPA, array-CGH, or other methods to establish sufficient coverage for its mutations.

The present analysis showed co-segregation of symptoms and *ELN* mutations in the majority of analyzed individuals. The three mutations identified in this study (c.370delT in family A, c.572-1G > A splice site in family B, and c.218_219insTG in family C) were highly pathogenic truncating mutations that result in premature stop codons (PTCs). A number of PTC mutations have actually been shown to be substrates of *ELN* mRNA insufficiency through nonsense-mediated decay in previous studies [17,21,35].

A highly variable phenotype within families with SVAS has been reported for large studies with many families with point mutations [20,21], and even for a family with apparently damaging 30 kb deletion involving multiple exons [7], ranging from asymptomatic mutation carrier to severe stenosis with multiple arteries. There were also two asymptomatic persons carrying *ELN* mutations (A:II-3 and C:II-3) in the present study. Factors affecting the variability of cardiovascular phenotypes in patients with *ELN* mutation are not yet fully understood, and there has as yet been no clear genotype-phenotype correlation reported for SVAS. Our comprehensive list of reported pathogenic SVAS mutations and deletions showed a universal distribution of variants over the entire *ELN* gene with no significant hotspot.

The primary mechanism for the pathogenesis of SVAS is proposed to be haploinsufficiency of *ELN*, as hemizygosity of *ELN* is established as the mechanism of SVAS in WBS [5]. Incomplete penetrance and a broad range in severity of cardiovascular phenotype are also seen in patients with WBS in whom one copy of *ELN* gene is totally lost [42,43]. Among possible causes affecting the severity of symptoms, the effect of the mutations in the remaining allele of *ELN* is very limited, as only two rare missense changes were identified through exon sequencing of 49 patients with WBS [44]. Currently, there is no definite explanation for the phenotypic variability associated with *ELN* mutations.

The present study showed that microdeletions of *ELN* gene could account for additional cases, around a half of previously unexplained cases, of familial SVAS, which would strengthen the causative role of *ELN* mutations in this disease entity. Therefore, quantitative genetic tests such as MLPA or array-CGH of *ELN* gene should be performed to genetically diagnose patients with familial SVAS to obtain satisfactory sensitivity. Further investigations of a larger cohort and so-far unexplained cases will be needed to elucidate the remaining molecular pathogenetic mechanisms of SVAS.

Supplementary data to this article can be found online at https://doi.org/10.1016/j.ijcard.2018.09.032.

Authors' contributions

All authors developed the concept and designed the research; S.H., Y.O., and M.T. performed the experiments; S.H., Y.O., M.T., H.I., H.K., and T.K. analyzed the data; all authors interpreted the results of the experiments; S.H., Y.O., and T.K. prepared the figures; S.H., Y.O., M.T., H.I., Y.F., H.K., S.K., Y.T., and T.K. drafted the manuscript; S.H., Y.O., and T.K. edited the manuscript; all authors approved the final version of the manuscript.

Source of funding

This work was supported by funding from the Morinaga Foundation for Health and Nutrition to Dr. Taichi Kato. The funders had no role in study design, data collection and analysis, decision to publish, or preparation of the manuscript.

Competing interests

The authors report no relationships that could be construed as a conflict of interest.

Acknowledgements

The authors would like to thank all of the clinicians and families who made this study possible with the provision of samples. The authors would also like to thank Dr. Shinsuke Kataoka (Department of Pediatrics, Nagoya University Graduate School of Medicine, Nagoya, Japan) for valuable assistance. The authors would also like to express their great appreciation to Drs. Sayaka Mii, Daichi Fukumi, Tameo Hatano (Department of Pediatrics, Japanese Red Cross Nagoya Daiichi Hospital, Nagoya, Japan), Takahiro Okumura (Department of Cardiology, Nagoya University Graduate School of Medicine), Kentaro Omoya, Takashi Kuwahara (Department of Pediatric Cardiology, Gifu Prefectural General Medical Center, Gifu, Japan), Naoki Ohashi, Hiroshi Nishikawa, Masaki Matsushima (Department of Pediatric Cardiology, Chukyo Hospital, Nagoya, Japan), Takaya Ota, Kenji Kuraishi, Nobuo Tauchi (Department of Pediatric Cardiology and Neonatology, Ogaki Municipal Hospital, Ogaki, Japan), and Noriko Nagai (Department of Pediatrics, Okazaki City Hospital, Okazaki, Japan) for their assistance with the collection of our samples and data. The authors would like to thank the Division for Medical Research Engineering, Nagoya University Graduate School of Medicine for technical support in next-generation sequencing. The authors also acknowledge the assistance of the Human Genome Center, Institute of Medical Science, University of Tokyo (http://sc.hgc.jp/shirokane.html), for providing supercomputing resources.

References

[1] A.K. Ewart, C.A. Morris, G.J. Ensing, J. Loker, C. Moore, M. Leppert, et al., A human vascular disorder, supravalvular aortic stenosis, maps to chromosome 7, Proc. Natl. Acad. Sci. U. S. A. 90 (1993) 3226–3230.
[2] A.J. Beuren, C. Schulze, P. Eberle, D. Harmjanz, J. Apitz, The syndrome of supravalvular aortic stenosis, peripheral pulmonary stenosis, mental retardation and similar facial appearance, Am. J. Cardiol. 13 (1964) 471–483.
[3] R. Eisenberg, D. Young, B. Jacobson, A. Boito, Familial supravalvular aortic stenosis, Am. J. Dis. Child. 108 (1964) 341–347.
[4] J.C. Williams, B.G. Barratt-Boyes, J.B. Lowe, Supravalvular aortic stenosis, Circulation 24 (1961) 1311–1318.
[5] B.R. Pober, Williams–Beuren syndrome, N. Engl. J. Med. 362 (2010) 239–252.
[6] J.M.Z.J. Frieland-Little, R.J. Gajarski, Aortic stenosis, in: H.D.S.R. Allen, D.J. Penny, T.F. Feltes, F. Cetta (Eds.), Moss & Adams Heart Disease in Infants, Children, and Adolescents: Including the Fetus and Young Adult, 9th edWolters Kluwer, Philadelphia 2016, pp. 1085–1105.
[7] D.Y. Li, A.E. Toland, B.B. Boak, D.L. Atkinson, G.J. Ensing, C.A. Morris, et al., Elastin point mutations cause an obstructive vascular disease, supravalvular aortic stenosis, Hum. Mol. Genet. 6 (1997) 1021–1028.
[8] T.M. Olson, V.V. Michels, Z. Urban, K. Csiszar, A.M. Christiano, D.J. Driscoll, et al., A 30 kb deletion within the elastin gene results in familial supravalvular aortic stenosis, Hum. Mol. Genet. 4 (1995) 1677–1679.
[9] A.K. Ewart, W. Jin, D. Atkinson, C.A. Morris, M.T. Keating, Supravalvular aortic stenosis associated with a deletion disrupting the elastin gene, J. Clin. Invest. 93 (1994) 1071–1077.
[10] M.E. Curran, D.L. Atkinson, A.K. Ewart, C.A. Morris, M.F. Leppert, M.T. Keating, The elastin gene is disrupted by a translocation associated with supravalvular aortic stenosis, Cell 73 (1993) 159–168.
[11] A.M. Jelsig, Z. Urban, V. Hucthagowder, H. Nissen, L.B. Ousager, Novel ELN mutation in a family with supravalvular aortic stenosis and intracranial aneurysm, Eur. J. Med. Genet. 60 (2017) 110–113.
[12] A. Jakob, S. Unger, R. Arnold, J. Grohmann, C. Kraus, C. Schlensak, et al., A family with a new elastin gene mutation: broad clinical spectrum, including sudden cardiac death, Cardiol. Young 21 (2011) 62–65.
[13] J. Katumba-Lunyenya, Two generations of identical twins with ELN deletion, BMJ Case Rep. 2009 (2009) (bcr06.2008.0036).
[14] M. Martin, S. Secades, A.M. Plasencia, M.L. Rodriguez, C. Corros, A. Garcia-Campos, et al., Supravalvular aortic stenosis as a non-syndromic familial disease. Relevance of familial screening, Int. J. Cardiol. 172 (2014) 511–512.
[15] G.M. Blue, E.P. Kirk, E. Giannoulatou, S.L. Dunwoodie, J.W. Ho, D.C. Hilton, et al., Targeted next-generation sequencing identifies pathogenic variants in familial congenital heart disease, J. Am. Coll. Cardiol. 64 (2014) 2498–2506.
[16] T.M. Olson, V.V. Michels, N.M. Lindor, G.M. Pastores, J.L. Weber, D.J. Schaid, et al., Autosomal dominant supravalvular aortic stenosis: localization to chromosome 7, Hum. Mol. Genet. 2 (1993) 869–873.
[17] Z. Urbán, V.V. Michels, S.N. Thibodeau, E.C. Davis, J.-P. Bonnefont, A. Munnich, et al., Isolated supravalvular aortic stenosis: functional haploinsufficiency of the elastin gene as a result of nonsense-mediated decay, Hum. Genet. 106 (2000) 577–588.
[18] D.Y. Li, G. Faury, D.G. Taylor, E.C. Davis, W.A. Boyle, R.P. Mecham, et al., Novel arterial pathology in mice and humans hemizygous for elastin, J. Clin. Invest. 102 (1998) 1783–1787.
[19] D.Y. Li, B. Brooke, E.C. Davis, R.P. Mecham, L.K. Sorensen, B.B. Boak, et al., Elastin is an essential determinant of arterial morphogenesis, Nature 393 (1998) 276–280.

[20] K. Metcalfe, A.K. Rucka, L. Smoot, G. Hofstadler, G. Tuzler, P. McKeown, et al., Elastin: mutational spectrum in supravalvular aortic stenosis, Eur. J. Hum. Genet. 8 (2000) 955–963.
[21] L. Micale, M.G. Turturo, C. Fusco, B. Augello, L.A. Jurado, C. Izzi, et al., Identification and characterization of seven novel mutations of elastin gene in a cohort of patients affected by supravalvular aortic stenosis, Eur. J. Hum. Genet. 18 (2010) 317–323.
[22] H. Muramatsu, Y. Okuno, K. Yoshida, Y. Shiraishi, S. Doisaki, A. Narita, et al., Clinical utility of next-generation sequencing for inherited bone marrow failure syndromes, Genet. Med. 19 (2017) 796–802.
[23] H. Li, R. Durbin, Fast and accurate short read alignment with burrows-wheeler transform, Bioinformatics 25 (2009) 1754–1760.
[24] D.C. Koboldt, Q. Zhang, D.E. Larson, D. Shen, M.D. McLellan, L. Lin, et al., VarScan 2: somatic mutation and copy number alteration discovery in cancer by exome sequencing, Genome Res. 22 (2012) 568–576.
[25] K. Wang, M. Li, H. Hakonarson, ANNOVAR: functional annotation of genetic variants from high-throughput sequencing data, Nucleic Acids Res. 38 (2010) e164.
[26] S. Richards, N. Aziz, S. Bale, D. Bick, S. Das, J. Gastier-Foster, et al., Standards and guidelines for the interpretation of sequence variants: a joint consensus recommendation of the American College of Medical Genetics and Genomics and the Association for Molecular Pathology, Genet. Med. 17 (2015) 405–424.
[27] Exome Variant Server, NHLBI GO Exome Sequencing Project (ESP). Seattle, WA, http://evs.gs.washington.edu/EVS/, Accessed date: 22 August 2017.
[28] C. Genomes Project, A. Auton, L.D. Brooks, R.M. Durbin, E.P. Garrison, H.M. Kang, et al., A global reference for human genetic variation, Nature 526 (2015) 68–74.
[29] M. Lek, K. Karczewski, E. Minikel, K. Samocha, E. Banks, T. Fennell, et al., Analysis of protein-coding genetic variation in 60,706 humans, bioRxiv, 2015.
[30] K. Higasa, N. Miyake, J. Yoshimura, K. Okamura, T. Niihori, H. Saitsu, et al., Human genetic variation database, a reference database of genetic variations in the Japanese population, J. Hum. Genet. 61 (2016) 547–553.
[31] J.J. Louw, G. Verleden, M. Gewillig, K. Devriendt, Haploinsufficiency of elastin gene may lead to familial cardiopathy and pulmonary emphysema, Am. J. Med. Genet. A 158a (2012) 2053–2054.
[32] X. Ge, Y. Ren, O. Bartulos, M.Y. Lee, Z. Yue, K.Y. Kim, et al., Modeling supravalvular aortic stenosis syndrome with human induced pluripotent stem cells, Circulation 126 (2012) 1695–1704.
[33] S. Park, E.J. Seo, H.W. Yoo, Y. Kim, Novel mutations in the human elastin gene (ELN) causing isolated supravalvular aortic stenosis, Int. J. Mol. Med. 18 (2006) 329–332.
[34] L. Rodriguez-Revenga, C. Badenas, A. Carrio, M. Mila, Elastin mutation screening in a group of patients affected by vascular abnormalities, Pediatr. Cardiol. 26 (2005) 827–831.
[35] Z. Urban, S. Riazi, T.L. Seidl, J. Katahira, L.B. Smoot, D. Chitayat, et al., Connection between elastin haploinsufficiency and increased cell proliferation in patients with supravalvular aortic stenosis and Williams-Beuren syndrome, Am. J. Hum. Genet. 71 (2002) 30–44.
[36] J. Dedic, A.S. Weiss, J. Katahira, B. Yu, R.J. Trent, Z. Urban, A novel elastin gene mutation (1281delC) in a family with supravalvular aortic stenosis: a mutation cluster within exon 20, Hum. Mutat. 17 (2001) 81.
[37] T. Boeckel, A. Dierks, A. Vergopoulos, S. Bahring, H. Knoblauch, B. Muller-Myhsok, et al., A new mutation in the elastin gene causing supravalvular aortic stenosis, Am. J. Cardiol. 83 (1999) 1141–1143 (a9–10).
[38] M. Tassabehji, K. Metcalfe, D. Donnai, J. Hurst, W. Reardon, M. Burch, et al., Elastin: genomic structure and point mutations in patients with supravalvular aortic stenosis, Hum. Mol. Genet. 6 (1997) 1029–1036.
[39] C. Stamm, I. Friehs, S.Y. Ho, A.M. Moran, R.A. Jonas, P.J. del Nido, Congenital supravalvar aortic stenosis: a simple lesion? Eur. J. Cardiothorac. Surg. 19 (2001) 195–202.
[40] G. Merla, N. Brunetti-Pierri, P. Piccolo, L. Micale, M.N. Loviglio, Supravalvular aortic stenosis: elastin arteriopathy, Circ. Cardiovasc. Genet. 5 (2012) 692–696.
[41] Z. Urban, J. Zhang, E.C. Davis, G.K. Maeda, A. Kumar, H. Stalker, et al., Supravalvular aortic stenosis: genetic and molecular dissection of a complex mutation in the elastin gene, Hum. Genet. 109 (2001) 512–520.
[42] L. Li, L. Huang, Y. Luo, X. Huang, S. Lin, Q. Fang, Differing microdeletion aizes and breakpoints in chromosome 7q11.23 in Williams-Beuren syndrome detected by chromosomal microarray analysis, Mol. Syndromol. 6 (2016) 268–275.
[43] A. Wessel, R. Pankau, D. Kececioglu, W. Ruschewski, J.H. Bursch, Three decades of follow-up of aortic and pulmonary vascular lesions in the Williams-Beuren syndrome, Am. J. Med. Genet. 52 (1994) 297–301.
[44] M. Delio, K. Pope, T. Wang, J. Samanich, C.R. Haldeman-Englert, P. Kaplan, et al., Spectrum of elastin sequence variants and cardiovascular phenotypes in 49 patients with Williams-Beuren syndrome, Am. J. Med. Genet. A 161A (2013) 527–533.

BMC Medical Genetics

CASE REPORT Open Access

Exonic duplication of the *OTC* gene by a complex rearrangement that likely occurred via a replication-based mechanism: a case report

Katsuyuki Yokoi[1,2], Yoko Nakajima[1], Hidehito Inagaki[2], Makiko Tsutsumi[2], Tetsuya Ito[1] and Hiroki Kurahashi[2*]

Abstract

Background: Ornithine transcarbamylase deficiency (OTCD) is an X-linked recessive disorder involving a defect in the urea cycle caused by *OTC* gene mutations. Although a total of 417 disease-causing mutations in *OTC* have been reported, structural abnormalities in this gene are rare. We here describe a female OTCD case caused by an exonic duplication of the *OTC* gene (exons 1–6).

Case presentation: A 23-year-old woman with late-onset OTCD diagnosed by biochemical testing was subjected to subsequent genetic testing. Sanger sequencing revealed no pathogenic mutation throughout the coding exons of the *OTC* gene, but multiplex ligation-dependent probe amplification (MLPA) revealed duplication of exons 1–6. Further genetic analyses revealed an inversion of duplicated exon 1 and a tandem duplication of exons 2–6. Each of the junctions of the inversion harbored a microhomology and non-templated microinsertion, respectively, suggesting a replication-based mechanism. The duplication was also of de novo origin but segregation analysis indicated that it took place in the paternal chromosome.

Conclusion: We report the first OTCD case harboring an exonic duplication in the *OTC* gene. The functional defects caused by this anomaly were determined via structural analysis of its complex rearrangements.

Keywords: Ornithine transcarbamylase deficiency, Exonic duplication, Complex rearrangement, Fork stalling and template switching (FoSTeS), Non-homologous end joining (NHEJ)

Background

Ornithine transcarbamylase (OTC) is a mitochondrial urea cycle enzyme that catalyzes the reaction between carbamyl phosphate and ornithine to form citrulline and phosphate [1]. Ornithine transcarbamylase deficiency (OTCD) is one of the most common urea cycle disorders [2] with an estimated prevalence of 1 in 14,000–77,000 [1]. The human *OTC* gene, located on the short arm of the X chromosome (Xp11.4), is 73 kb with10 exons and 1062 bp of coding sequence [3–5]. Because OTCD is inherited in an X-linked manner, deficient hemizygous males usually develop this disorder. However, a remarkable feature of OTCD is that a substantial subset of heterozygous females also develop this condition. The symptoms of carrier females vary in terms of onset and severity. Since the *OTC* gene is subject to X-inactivation, it is believed that this phenotypic variability depends on a skewed degree of this in the livers of carrier females [5].

In 85–90% of patients with a biochemical phenotype of OTCD, a mutation can be identified through sequencing or deletion/duplication testing [6]. A total of 417 disease-causing mutations in the *OTC* gene have been reported to date [1]. Exonic deletions have also been described but no prior case of OTCD caused by exonic duplication has previously been reported [7]. In our current case report, we describe a female patient with OTCD caused by a partial duplication of *OTC* exons 1–6.

* Correspondence: kura@fujita-hu.ac.jp
[2]Division of Molecular Genetics, Institute for Comprehensive Medical Science, Fujita Health University, 1-98 Dengakugakubo, Kutsukake-cho, Toyoake, Aichi 470-1192, Japan
Full list of author information is available at the end of the article

Case presentation

Patient

The current study patient was a 23-year-old woman with normal psychomotor development and healthy nonconsanguineous parents. She had frequent episodes of nausea, vomiting, stomachache and temporary elevated transaminase from about 4 years of age. Ammonia and plasma amino acid levels were measured when she was 5 years old. Her serum ammonia was 220 μg/dl (normal range 12 ~ 60 μg/dl) and she showed high levels of glutamine (1212 nmol/ml; normal value, 420–700), lower normal limits of citrulline (18.4 nmol/ml; normal value, 17–43), and lower plasma levels of arginine (32.2 nmol/ml; normal value, 54–130). A urine metabolic screen indicated a gross elevation in orotate (orotate/creatinine ratio 234.3 μmol/g creatinine; normal value, 4.7 ~ 15.9 μmol/g creatinine). These findings were consistent with OTC deficiency. She was therefore biochemically diagnosed with OTCD and her blood ammonia level has been well controlled since by a protein-restricted diet and by oral sodium phenylbutyrate and arginine. Recently, we performed genetic analysis to identify the genetic alterations of the *OTC* gene in this patient. However, Sanger sequencing revealed no pathogenic mutation.

Genetic analysis

Mutational analyses

Sanger sequencing was performed to screen for genetic variations at the nucleotide level throughout all coding exons of the *OTC* gene (Additional file 1). We used UCSC genome browser (http://genome-asia.ucsc.edu/) as human genome assembly. To screen for exonic deletions or duplications, multiplex ligation-dependent probe amplification (MLPA) was performed using the SALSA P079-A3 *OTC* MLPA kit (MRC Holland, Amsterdam, The Netherlands), in accordance with the manufacturer's recommendations. MLPA products were separated by capillary electrophoresis on an ABI3730 genetic analyzer and then processed using GeneMapper software. The peak heights of the samples were compared with control probes and the ratios of these peaks were calculated for all exons. If the dosage quotient was 1.0, the results were considered normal. Thresholds for deletions and duplications were set at 0.5 and 1.5, respectively.

Quantitative real time PCR

To demarcate the duplicated region, quantitative real-time PCR was conducted on blood DNA from the patient and a male control subject using the Applied Biosystems 7300 real time PCR system (Thermo Fisher Scientific). Several primer pairs were designed for *OTC* (upstream of exon 1 and intron 6) and *RPP30* that was used as an autosomal single copy gene reference to generate amplicons suitable for real-time PCR (Fig. 1b, Additional file 1). The PCR reaction was performed in a 15 μL reaction system, containing 2 μL of template DNA (5 ng/μL), 0.6 μL of each primer set (10 μmol/L), 0.3 μL ROX Reference Dye, 4 μL distilled water, and 7.5 μL of 2xTB Green Premix Ex TaqII (Tli RNaseH Plus, TaKaRa). Two parallel PCR reactions were prepared for each sample. The amplification cycling conditions were as follows: 95 °C for 30 s, followed by 40 cycles at 95 °C 5 s and 60 °C for 1 min. Data evaluation was carried out using the 7300 system SDS software and Microsoft Excel. The threshold cycle number (Ct) was determined for all PCR reactions and the same threshold and baseline were set for all samples. The starting copy number of the samples was determined using theΔΔCt-Method. ΔΔCt method was a modification of the method described in Livak et al. for quantifying mRNA [8]. ΔCt represents the mean Ct value of each sample and was calculated for *OTC* and *RPP30*. The starting copy number of the unknown samples was determined relative to the known copy number of the control sample using the following formula:

ΔΔCt = [ΔCt OTC(patient)-ΔCt RPP30(patient)] - [ΔCt OTC(female)-ΔCt RPP30(female)]. The relative gene copy number was calculated by the expression $2^{-\Delta(\Delta Ct)}$. The starting copy number of male control was also determined as a reference value.

Inverse PCR

Inverse PCR were performed using restriction enzyme *Taq*I (TaKaRa, Shiga, Japan) to isolate the unknown sequences adjacent to the duplicated region of the *OTC* gene in the study patient. ApE – A plasmid Editor software was used to identify the recognition sites for the restriction enzyme. The restriction enzyme was chosen based on the following criteria: (1) no cutting of the expected breakpoint area; and (2) endonuclease activity would be unaffected by CpG methylation of the target sequence. A 100 ng aliquot of genomic DNA from both our patient and a control female was digested with the selected restriction enzyme in a total volume of 30 μl at 65 °C for 90 min. The reaction was inactivated using the QiaQuick PCR Purification Kit. A 20 μL sample of digested DNA was then mixed with 23 μL of DW, 5 μL of 10 × T4 ligase buffer (TaKaRa, Shiga, Japan) and 2 μL of T4 DNA ligase to make a final volume of 50 μL. Ligation reactions were incubated at 16 °C for 16 h. For subsequent PCR, 1 μL of digested and re-ligated DNA template was used in a total reaction volume of 25 μL with Tks Gflex DNA Polymerase (TaKaRa, Shiga, Japan). Primers were designed to avoid repetitive sequences (Additional file 1). The PCR conditions were as follows: 30 cycles of 10 s at 98 °C, 15 s at 60 °C, and 1 min at 68 °C. Amplified products were analyzed by gel

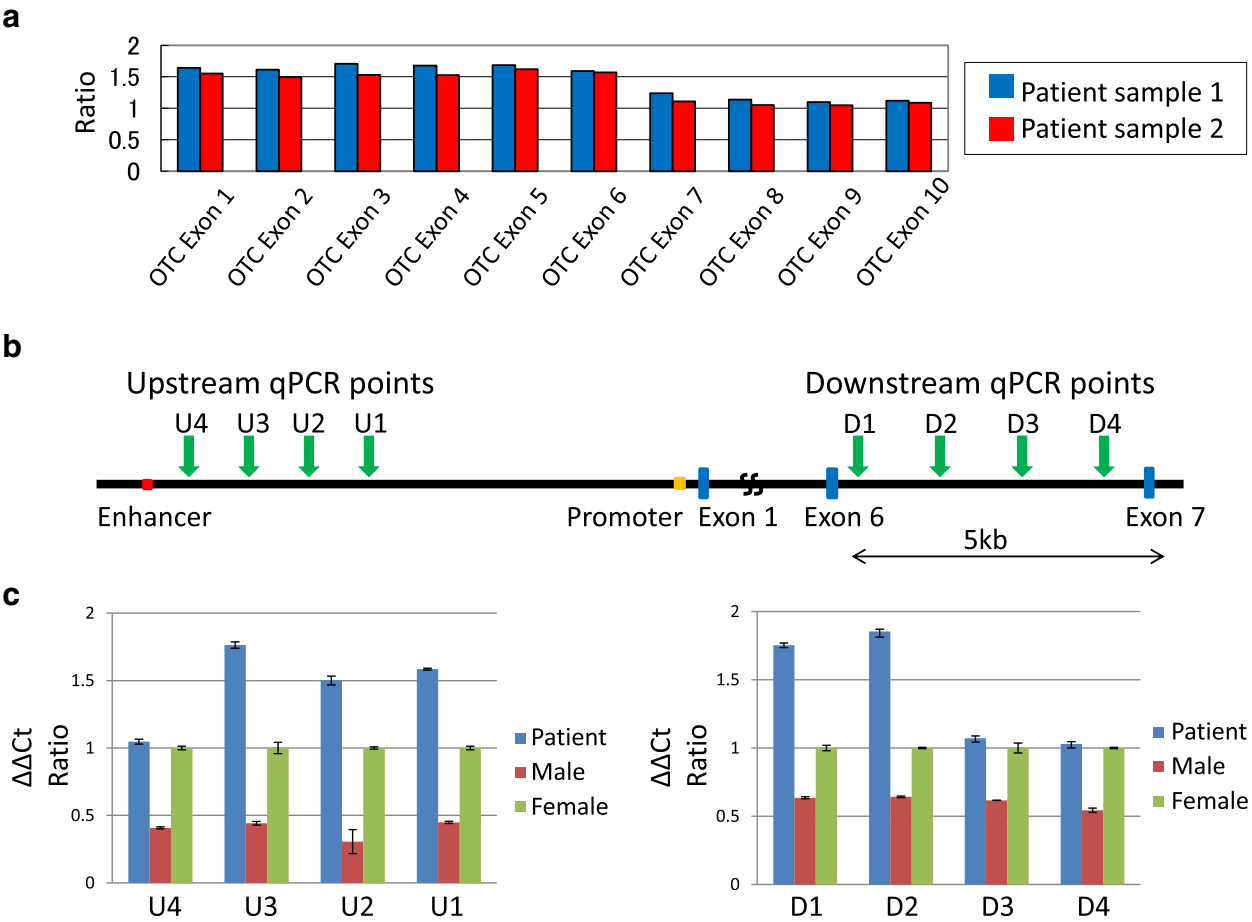

Fig. 1 Exonic duplication of the *OTC* gene in a female OTCD patient. **a** MLPA results for the *OTC* gene in this patient indicting duplication of exons 1–6. **b** Structure of the *OTC* gene. The blue boxes denote exons. The enhancer and promoter regions are shown in red and orange, respectively. The positions of the qPCR units are indicated by green arrows. Upstream qPCR units: U1 - U4. Downstream qPCR units: D1 - D4. **c** qPCR results. The left and right panels show the qPCR findings for the upstream and downstream regions, respectively. The blue bars indicate the patient and the red and green bars denote the male and female controls, respectively. The Y- axis indicates the **ΔΔ** Ct ratio

electrophoresis and were purified following nested PCR (Additional file 1). The purified PCR products were sequenced via the standard Sanger method.

Breakpoint analysis on the other side

PCR was performed using Tks Gflex (TaKaRa, Shiga, Japan) to confirm the other side of the breakpoint sequence. Primer R which was previously designed for real-time PCR analysis of *OTC* upstream of exon 1 (i.e. *OTC* intron 1) was used as primer F in this reaction (Additional file 1). The PCR conditions and Sanger methodology were similar to those described above.

MLPA revealed the duplication of exons 1–6 of the *OTC* gene in our current study patient (Fig. 1a). We determined the range of the duplication using quantitative real-time PCR (Fig. 1b). We designed four qPCR experiments (U1-U4) between the promoter and enhancer regions to identify the upstream breakpoint. Likewise, we designed four qPCR assays (D1-D4) within intron 6 to identify the downstream breakpoint. In contrast to the male or female controls that showed ΔΔCt ratios of 0.5 or 1.0, respectively, the patient's samples showed aΔΔCt ratio > 1.5 in some of these qPCR assays, suggesting that these regions were duplicated in this patient (Fig. 1c). The results indicated that the putative upstream breakpoints were located between PCR U3 and U4, and that the downstream breakpoints were between PCR D2 and D3.

We next performed inverse PCR to analyze the genomic structure of the duplicated region. *Taq*I-digested DNA was used as a template to produce a 3.5 kb PCR product when amplified with inversely oriented intron 6 primers (Fig. 2a, c). However, an additional small PCR product was detected by agarose gel electrophoresis in the patient sample (Fig. 2a). The amplified products were sequenced after nested PCR (Fig. 2a). As expected,

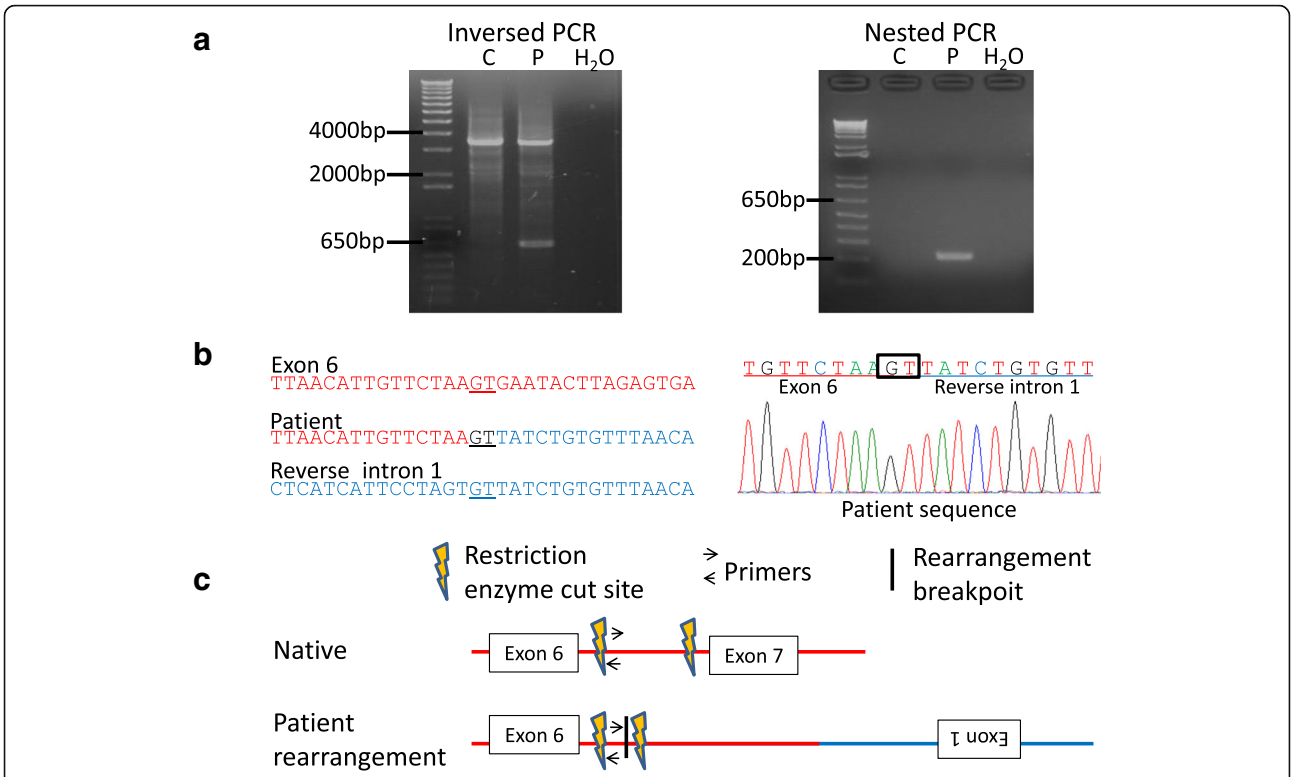

Fig. 2 Identification of the duplication junction via inverse PCR. **a** Isolation of the junction fragment. Two distinct inverse PCR products were observed following agarose gel electrophoresis. The larger product was derived from a normal allele and the small product from a rearranged allele (left). The amplified products were purified following nested PCR (right). P, patient; C, control; H, H_2O. **b** Sanger sequencing of the PCR products including the junction. The unknown sequence next to the junction was identified as intron 1 of the *OTC* gene in the reverse orientation. The normal exon 6 and intron 1 sequences are aligned in red and blue typeface, respectively. Underlined nucleotides indicate microhomology at the breakpoint junction. **c** Predicted structure of the junction. Horizontal arrows indicate the recognition sites of the primers used for inverse PCR and the vertical arrows denote the *Taq*I restriction sites

the breakpoint was located within intron 6 (Fig. 2b, c). Unexpectedly however, this breakpoint was found to be connected with intron 1 of the *OTC* gene in the reverse orientation. The breakpoint junction contained 2 nucleotides of microhomology at the fusion junction (Fig. 2b).

The other side breakpoint was analyzed using standard PCR with primers for the upstream breakpoint region and the breakpoint region in intron 1. The primer pair amplified only products from the patient's DNA (Fig. 3a). By Sanger sequencing, the upstream region of the *OTC* gene was found to make an inverted connection with 1 (Fig. 3b, c). This breakpoint junction contained an additional 4 nucleotides (ACTA) of unknown origin (Fig. 3b). The positions of the two breakpoints in intron 1 were found to be chrX: 38365292 and chrX: 38366694, which were 1402 bp apart (Fig. 3c). We performed the same PCR amplification of both junctions in the patient's parents but detected no products, suggesting that this complex rearrangement arose de novo. The patient's duplicated region included a common single nucleotide variant (rs752750694, NM_000531.5:c.-844C > T). The patient's father carries an A whereas the mother carries a G/G at this site (Fig. 3d). The patient was found to be an A/G heterozygote, but the peak of the A nucleotide was two-fold greater than the G-peak, suggesting that the patient carries two copies of A. These data suggest that the de novo duplication was of paternal origin.

Discussion and conclusions

We here report the first documented case of OTCD caused by an exonic duplication of the *OTC* gene. Although the MLPA results for this case indicated a simple duplication of exons 1–6, further analysis indicated that it resulted from complex rearrangements. Two possible mechanisms have been proposed for such rearrangements: one is chromothripsis that is caused by chromosome shuttering followed by reunion, and the other is chromoanasynthesis that is a replication-based mechanism also known as fork stalling and template switching (FoSTeS)/microhomology-mediated break-induced replication (MMBIR). According to the replication-based model, the active replication fork can stall and switch templates using complementary template microhomology to anneal and prime DNA replication. This

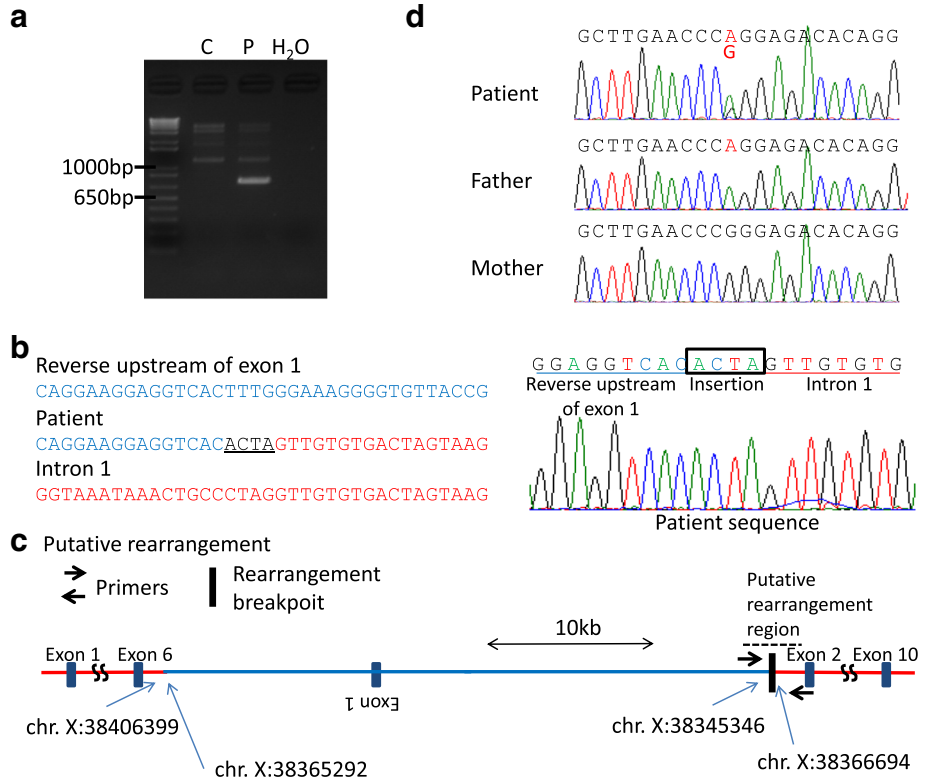

Fig. 3 The complex rearrangement in the *OTC* gene of the study patient likely occurred via a replication-based mechanism. **a** Identification of the other junction by PCR. The PCR primer pair successfully amplified the junction product only from the OTCD study patient DNA. P, patient; C, control; H, H_2O. **b** Sanger sequencing results for the PCR products including the junction. The normal sequence of the *OTC* gene upstream region and intron 1 are aligned in blue and red typeface, respectively. Underlined bases denote a non-templated microinsertion at the junction. **c** Predicted structure of the complex rearrangement leading to the *OTC* gene duplication. The positions of the PCR primers are indicated by black arrows. The first junction is indicated by a blue arrow. The nucleotide position of the breakpoints on the X-chromosome are also indicated. The position of the two breakpoints in intron 1 were found to be chr. X: 38365292 and chr. X: 38366694, which were 1402 bp apart. **d** Trio-genotyping of the common single nucleotide variant (rs752750694, NM 000531.5:c.-844C > T). The patient's father carries A and her mother carries G/G. The patient was found to be an A/G heterozygote, but her A peak was two-fold higher than the G-peak. The areas under the curve (AUC) were 900 (A) and 328 (G) (Image J)

mechanism enables the joining or template-driven juxtaposition of different sequences from discrete genomic positions and can result in complex rearrangements [9].

In our current OTCD case, one junction presented 2 nucleotides of microhomology (GT), and the other junction manifested 4 nucleotides as a microinsertion (ACTA). Copy number variation with complex rearrangements and the presence of microhomology is indicative of a replication-based mechanism but the evidence for a non-templated microinsertion is noteworthy. Microinsertions are often observed in non-proofing DNA repair processes such as non-homologous end joining (NHEJ), which is activated by double-strand breaks [10]. However, a considerable body of evidence now suggests that microinsertions can be identified at junctions mediated by DNA replication-based mechanisms [11, 12]. A recent study has also suggested that an NHEJ-like pathway mediated by Polθ, which is an alternative NHEJ mechanism, may be induced by replication stress [13]. Taken together, an alternative NHEJ pathway might be activated during aberrant replication to restore DNA integrity, thus leading to chromoanasynthesis.

The evidence to date also suggests that de novo mutations occur more frequently in paternal alleles [14]. This bias is attributed to the higher number of DNA replication events in spermatogenesis than in oogenesis. Likewise, chromosomal structural variations are more frequently derived from the father [15]. The complex genomic rearrangements in our present patient were found to be of de novo origin but genotyping of a single nucleotide variant in the *OTC* gene demonstrated that the rearrangement allele originated from her father. Given the higher chance of the DNA replication errors during spermatogenesis, it might also reflect the replication-based mechanism.

MLPA can be used in the molecular diagnosis of several genetic diseases whose pathogenesis is related to the presence of deletions or duplications of specific genes [16]. Although deletions are clearly pathogenic, this is less certain in the case of duplications. In case of the

OTC gene for example, duplications of the entire gene are innocuous and present as a normal variant in the general population [7]. In cases of partial duplication as seen in our current patient, gene function may not be necessarily be affected when the additional sequence is inserted into another genomic locus. Even in cases of a tandem duplication, it is feasible that one copy of the *OTC* gene may maintain an intact structure. In the current OTCD case, the inversion of exon 1 occurred together with its duplication. We predicted in this instance that this complex rearrangement would generate a tandem duplication of exons 2–6 and the production of truncated OTC proteins with defective function due to a frameshift or null protein expression due to nonsense-mediated mRNA decay. The functional defects caused by this mutant allele were therefore the cause of the OTCD in this woman.

In conclusion, we report the first case of OTCD caused by a complex rearrangement resulting in exonic duplication of the *OTC* gene. Our present report also emphasizes the necessity of fully investigating whether pathogenicity has resulted from a genomic duplication.

Additional file

Additional file 1: PCR primers and genomic coordinates. (a) Primers for Sanger sequences of *OTC* exons. (b) Primers for qRT-PCR. (c) Other PCR. (XLSX 13 kb)

Abbreviations

FoSTeS: Fork stalling and template switching; MLPA: Multiplex ligation-dependent probe amplification; MMBIR: Microhomology-mediated break-induced replication; NHEJ: Non-homologous end joining; OTC: Ornithine transcarbamylase; OTCD: Ornithine transcarbamylase deficiency

Acknowledgements

We thank the patient and her family for their participation in this study. We also thank past and present members of our laboratory.

Funding

No funding was received.

Availability of data and materials

All data generated or analysed during this study are included in this published article [and its Additional files].

Authors' contributions

KY did most of the experiments, retrieved the data, drafted and revised the manuscript. YN and TI discovered the patients and provided many data. HI and MT supported and supervised experiments. HK have contributed equally to the manuscript. All authors contributed to and reviewed the manuscript. All authors read and approved the final manuscript.

Ethics approval and consent to participate

All procedures followed were in accordance with the ethical standards of the responsible committee on human experimentation (institutional and national) and with the Helsinki Declaration of 1975, as revised in 2005(5). The study protocol was approved by the Ethical Review Board for Human Genome Studies at Fujita Health University.

Consent for publication

Written informed consent to publish medical information and images was obtained from all patients reported in this publication.

Competing interests

The authors declare that they have no competing interests.

Publisher's Note

Author details

[1]Department of Pediatrics, Fujita Health University School of Medicine, Toyoake, Japan. [2]Division of Molecular Genetics, Institute for Comprehensive Medical Science, Fujita Health University, 1-98 Dengakugakubo, Kutsukake-cho, Toyoake, Aichi 470-1192, Japan.

Received: 13 September 2018 Accepted: 3 December 2018
Published online: 12 December 2018

References

1. Caldovic L, Abdikarim I, Narain S, Tuchman M, Morizono H. Genotype-phenotype correlations in ornithine Transcarbamylase deficiency: a mutation update. J Genet Genomics. 2015;42(5):181–94.
2. Seminara J, Tuchman M, Krivitzky L, Krischer J, Lee HS, Lemons C, et al. Establishing a consortium for the study of rare diseases: the urea cycle disorders consortium. Mol Genet Metab. 2010;100(Suppl 1):S97–105.
3. Lindgren V, de Martinville B, Horwich AL, Rosenberg LE, Francke U. Human ornithine transcarbamylase locus mapped to band Xp21.1 near the Duchenne muscular dystrophy locus. Science. 1984;226(4675):698–700.
4. Horwich AL, Fenton WA, Williams KR, Kalousek F, Kraus JP, Doolittle RF, et al. Structure and expression of a complementary DNA for the nuclear coded precursor of human mitochondrial ornithine transcarbamylase. Science. 1984;224(4653):1068–74.
5. Yorifuji T, Muroi J, Uematsu A, Tanaka K, Kiwaki K, Endo F, et al. X-inactivation pattern in the liver of a manifesting female with ornithine transcarbamylase (OTC) deficiency. Clin Genet. 1998;54(4):349–53.
6. Jang YJ, LaBella AL, Feeney TP, Braverman N, Tuchman M, Morizono H, et al. Disease-causing mutations in the promoter and enhancer of the ornithine transcarbamylase gene. Hum Mutat. 2018;39(4):527–36.
7. Shchelochkov OA, Li FY, Geraghty MT, Gallagher RC, Van Hove JL, Lichter-Konecki U, et al. High-frequency detection of deletions and variable rearrangements at the ornithine transcarbamylase (OTC) locus by oligonucleotide array CGH. Mol Genet Metab. 2009;96(3):97–105.
8. Livak KJ, Schmittgen TD. Analysis of relative gene expression data using real-time quantitative PCR and the 2(−Delta Delta C(T)) method. Methods. 2001;25(4):402–8.
9. Zhang F, Carvalho CM, Lupski JR. Complex human chromosomal and genomic rearrangements. Trends Genet. 2009a;25(7):298–307.
10. Lieber MR. The mechanism of human nonhomologous DNA end joining. J Biol Chem. 2008;283(1):1–5.
11. Hastings PJ, Lupski JR, Rosenberg SM, Ira G. Mechanisms of change in gene copy number. Nat Rev Genet. 2009;10(8):551–64.
12. Zhang F, Khajavi M, Connolly AM, Towne CF, Batish SD, Lupski JR. The DNA replication FoSTeS/MMBIR mechanism can generate genomic, genic and exonic complex rearrangements in humans. Nat Genet. 2009b;41(7):849–53.
13. Masset H, Hestand MS, Van Esch H, Kleinfinger P, Plaisancié J, Afenjar A, et al. A distinct class of Chromoanagenesis events characterized by focal copy number gains. Hum Mutat. 2016;37(7):661–8.
14. Jónsson H, Sulem P, Kehr B, Kristmundsdottir S, Zink F, Hjartarson E, et al. Parental influence on human germline de novo mutations in 1,548 trios from Iceland. Nature. 2017;549(7673):519–22.
15. Kurahashi H, Bolor H, Kato T, Kogo H, Tsutsumi M, Inagaki H, et al. Recent advance in our understanding of the molecular nature of chromosomal abnormalities. J Hum Genet. 2009;54(5):253–60.
16. Stuppia L, Antonucci I, Palka G, Gatta V. Use of the MLPA assay in the molecular diagnosis of gene copy number alterations in human genetic diseases. Int J Mol Sci. 2012;13(3):3245–76.

JIMD Reports
DOI 10.1007/8904_2018_108

RESEARCH REPORT

Disruption of the Responsible Gene in a Phosphoglucomutase 1 Deficiency Patient by Homozygous Chromosomal Inversion

Katsuyuki Yokoi • Yoko Nakajima • Tamae Ohye • Hidehito Inagaki • Yoshinao Wada • Tokiko Fukuda • Hideo Sugie • Isao Yuasa • Tetsuya Ito • Hiroki Kurahashi

Received: 13 February 2018 / Revised: 06 April 2018 / Accepted: 10 April 2018 / Published online: 12 May 2018

Abstract Phosphoglucomutase 1 (PGM1) deficiency is a recently defined disease characterized by glycogenosis and a congenital glycosylation disorder caused by recessive mutations in the *PGM1* gene. We report a case of a 12-year-old boy with first-cousin parents who was diagnosed with a PGM1 deficiency due to significantly decreased PGM1 activity in his muscle. However, Sanger sequencing revealed no pathogenic mutation in the *PGM1* gene in this patient. As this case presented with a cleft palate in addition to hypoglycemia and elevated transaminases and creatine kinase, karyotyping was performed and identified homozygous inv(1)(p31.1p32.3). Based on the chromosomal location of the *PGM1* gene at 1p31, we analyzed the breakpoint of the inversion. Fluorescence in situ hybridization (FISH) combined with long PCR analysis revealed that the inversion disrupts the *PGM1* gene within intron 1. Since the initiation codon in the *PGM1* gene is located within exon 1, we speculated that this inversion inactivates the *PGM1* gene and was therefore responsible for the patient's phenotype. When standard molecular testing fails to reveal a mutation despite a positive clinical and biochemical diagnosis, the presence of a gross structural variant that requires karyotypic examination must be considered.

Communicated by: Eva Morava, MD PhD

K. Yokoi · Y. Nakajima · T. Ito
Department of Pediatrics, Fujita Health University School of Medicine, Toyoake, Japan

K. Yokoi · T. Ohye · H. Inagaki · H. Kurahashi (✉)
Division of Molecular Genetics, Institute for Comprehensive Medical Science, Fujita Health University, Toyoake, Japan
e-mail: kura@fujita-hu.ac.jp

Y. Wada
Department of Obstetric Medicine, Osaka Women's and Children's Hospital, Osaka, Japan

T. Fukuda
Department of Pediatrics, Hamamatsu University School of Medicine, Hamamatsu, Japan

H. Sugie
Faculty of Health and Medical Sciences, Tokoha University, Hamamatsu, Japan

I. Yuasa
Division of Legal Medicine, Tottori University Faculty of Medicine, Yonago, Japan

H. Kurahashi
Genome and Transcriptome Analysis Center, Fujita Health University, Toyoake, Japan

H. Kurahashi
Center for Collaboration in Research and Education, Fujita Health University, Toyoake, Japan

Introduction

Phosphoglucomutase 1 (PGM1) deficiency is a recently defined disease, characterized by glycogenosis and a congenital disorder of glycosylation (CDG) (Tagtmeyer et al. 2014). ς PGM1 deficiency is rare with only 38 patients from 29 families with different ethnic backgrounds described in the literature so far (Perez et al. 2013; Ondruskova et al. 2014; Tagtmeyer et al. 2014; Loewenthal et al. 2015; Zeevaert et al. 2016; Wong et al. 2016; Preisler et al. 2017; Nolting et al. 2017; Voermans et al. 2017). PGM1 is an essential enzyme in carbohydrate biosynthesis and metabolism and functions both in glycogen synthesis and breakdown through a reversible conversion of glucose

1-phosphate to glucose 6-phosphate (Morava 2014). Since glucose 1-phosphate is a precursor of the nucleotide sugars used for glycan biosynthesis, PGM1 activity is also required for protein *N*-glycosylation (Beamer 2015). Hence, PGM1 deficiency has considerably diverse phenotypes. Most of the affected patients develop a congenital anomaly syndrome showing a bifid uvula, cleft palate, and Pierre Robin sequence as clinical manifestations from the time of birth. Hepatopathy, dilated cardiomyopathy (DCM), hypoglycemia, muscle weakness, exercise intolerance, growth retardation, and endocrine abnormalities emerge in these cases over time (Scott et al. 2014). Many of these manifestations can be linked to the role of PGM1 in glucose metabolism and glycosylation (Beamer 2015).

PGM1 deficiency is caused by homozygous or compound heterozygous nucleotide alterations in the *PGM1* gene (Herbich et al. 1985). Several types of mutations have been reported to date including missense mutations, frameshifts, and splicing mutations (Tagtmeyer et al. 2014; Lee et al. 2014; Perez et al. 2013; Timal et al. 2012; Stojkovic et al. 2009; Ondruskova et al. 2014). In our current report, we describe a case of PGM1 deficiency caused by a homozygous chromosomal inversion that disrupts the *PGM1* gene at chromosome 1p31.

Materials and Methods

Cytogenetic Analysis

Fluorescence in situ hybridization (FISH) analysis of the patient and his parents was performed using standard methods to detect the breakpoint region at the chromosome level. Briefly, phytohemagglutinin-stimulated lymphocytes or Epstein-Barr virus-transformed lymphoblastoid cell lines derived from the subjects were arrested by exposure to colcemid. Metaphase preparations were then obtained by hypotonic treatment with 0.075 M KCl followed by methanol/acetate fixation. A bacterial artificial clone (BAC) containing 1p31.1, RP4-534K7 (chr1:63,525,021-63,677,603), was used as the test probe, and a chromosome 1 centromere probe (CEN1 SpectrumOrange Probe; Abbott Laboratories, Abbott Park, IL) was used as a reference. The probes were labeled by nick translation with digoxigenin-11-dUTP. After hybridization, the probes were detected with DyLight 488 Anti-Digoxigenin/Digoxin. Chromosomes were visualized by counterstaining with 4,6-diamino-2-phenylindole.

Sequence Analysis

To isolate the breakpoint, long-range PCR with several sets of primers for the *PGM1* gene was performed using LA Taq (TaKaRa, Shiga, Japan) (Fig. 3c). The PCR conditions were 35 cycles of 10 s at 98°C and 15 min at 60°C. PCR primers were designed using sequence data from the human genome database. PCR products were separated on 0.8% (w/v) agarose gels and visualized with ethidium bromide. The homology between the obtained sequence around the breakpoint within the *PGM1* gene and the 1p32.3 sequence obtained from the database was examined using the BLAT in UCSC genome browser (http://genome-asia.ucsc.edu/human GRCh38/hg38).

Patient

The current study patient was a 12-year-old boy from consanguineous parents who are first cousins without a family history of congenital metabolic disease (Fig. 1). The patient's height was 137 cm (*z*-score −2.3), and he had a normal body weight of 39 kg (*z*-score −0.6). He was born at term with a normal body weight and length. A cleft palate was noted at birth and closure surgery was performed at 12 months. Persistently elevated transaminases (AST 50–400 U/L [normal value <33 U/L] and ALT 40–300 U/L [normal value <30 U/L]) had been observed since that surgery. In addition, mild hypoglycemia after overnight fasting and an occasionally elevated serum creatine kinase (100–2,600 U/L [normal value <287 U/L]) were evident from 2 years of age. The echocardiogram and electrocardiogram readings showed no abnormalities, and his psychomotor development was normal. Oral administration of uncooked corn starch prior to bedtime was commenced to prevent morning hypoglycemia.

At 2 years of age, the patient was referred to our department for further examination. Intravenous glucose loading at 2 g/kg led to an elevated lactate level (from 7 to 37 mg/dL at 120 min) with a normal lactate/pyruvate ratio. Intramuscular glucagon loading at 0.03 mg/kg caused no increase of blood sugar either during fasting or at 2 h after a meal, indicating a deficiency in the generation of hepatic glucose from glycogen. However, the activity of the debrancher enzyme responsible for glycogen storage disease (GSD) type III, phosphorylase involved in GSD type VI, and phosphorylase kinase enzyme associated with GSD type IX in the peripheral blood was normal. A forearm nonischemic exercise test was performed when the patient was 8 years old. No increase in venous lactate with a large elevation in his ammonia levels (297 μg/dL) was observed, suggesting inadequate glycogen utilization in the muscle. A muscle biopsy was therefore performed, and a significant decrease in PGM activity was identified (62.1 nmol/min/mg [controls 351.1 ± 81.1]). Isoelectric focusing (IEF) of serum transferrin was performed as previously described (Okanishi et al. 2008) and revealed a mixed type I and type II pattern, typical features of CDG-I and CDG-II (Fig. 2) (Tagtmeyer et al. 2014).

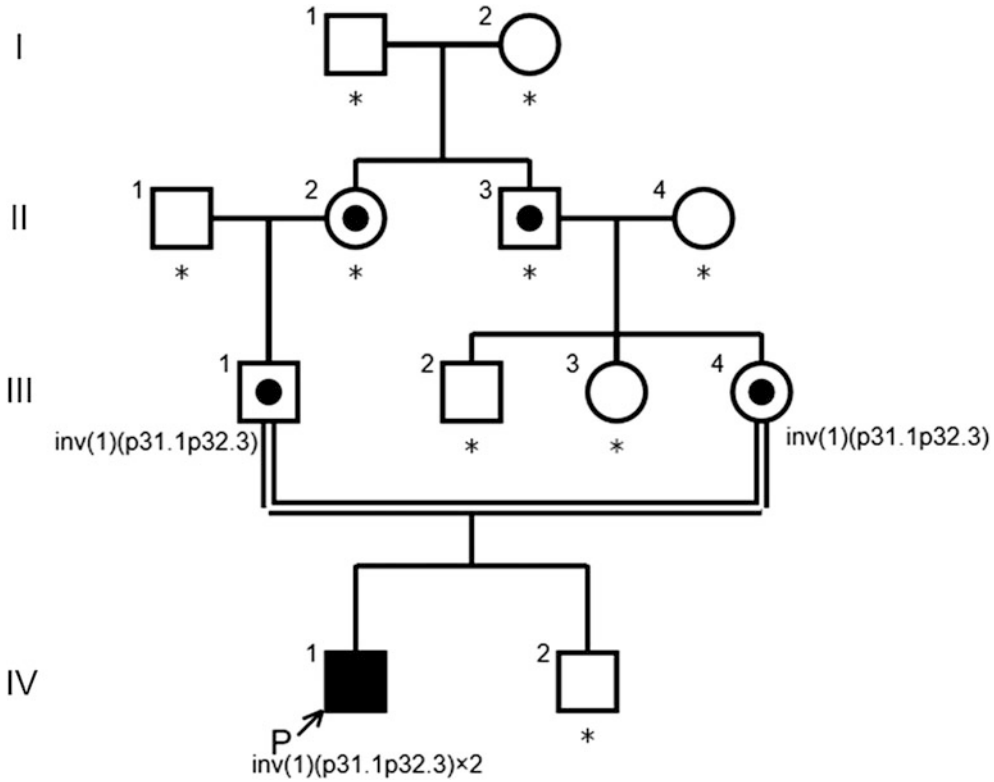

Fig. 1 Pedigree of the family. Arrow indicates proband. Carriers are represented by a dot in the middle of circles or squares. Asterisks indicate the family members who have not been tested

Mass spectrometry to characterize the molecular abnormality of transferrin was performed as previously described (Wada 2016) and further revealed the presence of a variety of transferrin glycoforms, including forms lacking one or both glycans as well as forms with truncated glycan (Fig. 2). These findings were consistent with a PGM1 deficiency (Tagtmeyer et al. 2014), and genetic analysis was performed to confirm this. Sanger sequencing revealed only c.1258T>C, a common polymorphism in the database. The karyotype of the patient was determined to be 46,XY, inv(1)(p31.1p32.3)x2, of which inv(1) was homozygous (Fig. 3a). Since the *PGM1* gene is localized at 1p31, we hypothesized that the inversion disrupts this gene in our patient, and we thus analyzed its distal breakpoint.

Results

FISH signals for the BAC RP4-534K7 probe that incorporates the entire *PGM1* gene are observed on the short arm of chromosome 1 in an individual with a normal karyotype. In our current study patient however, two distinct signals were detected on the short arm of both chromosome 1 homologues (Fig. 3b). This result indicated that the inversion breakpoint in the patient had disrupted the *PGM1* genomic region. Karyotype analysis of both parents showed 46,XY,inv(1)(p31.1p32.3). Both parents carried the inv(1) in a heterozygous state, suggesting that the two inv(1) homologues of the patient had been transmitted from each parent, respectively (data not shown).

Long PCR revealed that one of the PCR primer pairs (4F-4R) within intron 1 failed to amplify the products in the patient DNA, indicating that the breakpoint of the inversion was located in intron 1 (Fig. 3d). To analyze the breakpoint region in more detail, we performed additional long PCR. The 4F4-4R but not the 4F3-4R primer pair successfully yielded a PCR product. This indicated that the breakpoint was located between primer 4F3 and 4F4. We did not obtain the sequence of the other breakpoint region at 1p32.3. To ascertain the mechanism leading to the inversion, we obtained the sequence information of the 1p32.3 from the database and analyzed the homology with the 4F3-4F4 sequence. However, we did not find any sequence similarity between the 4F3-4F4 sequence and the genomic sequence at 1p32.3.

Discussion

PGM1 deficiency is a newly identified metabolic disorder which manifests features of both CDG and glycogenosis (Tagtmeyer et al. 2014). Our present case report describes a young male patient with PGM1 deficiency caused by a homozygous inv(1) inherited from his first-cousin parents that disrupts each of the two *PGM1* alleles. To date, 38 PGM1 deficiency patients have been reported, and patho-

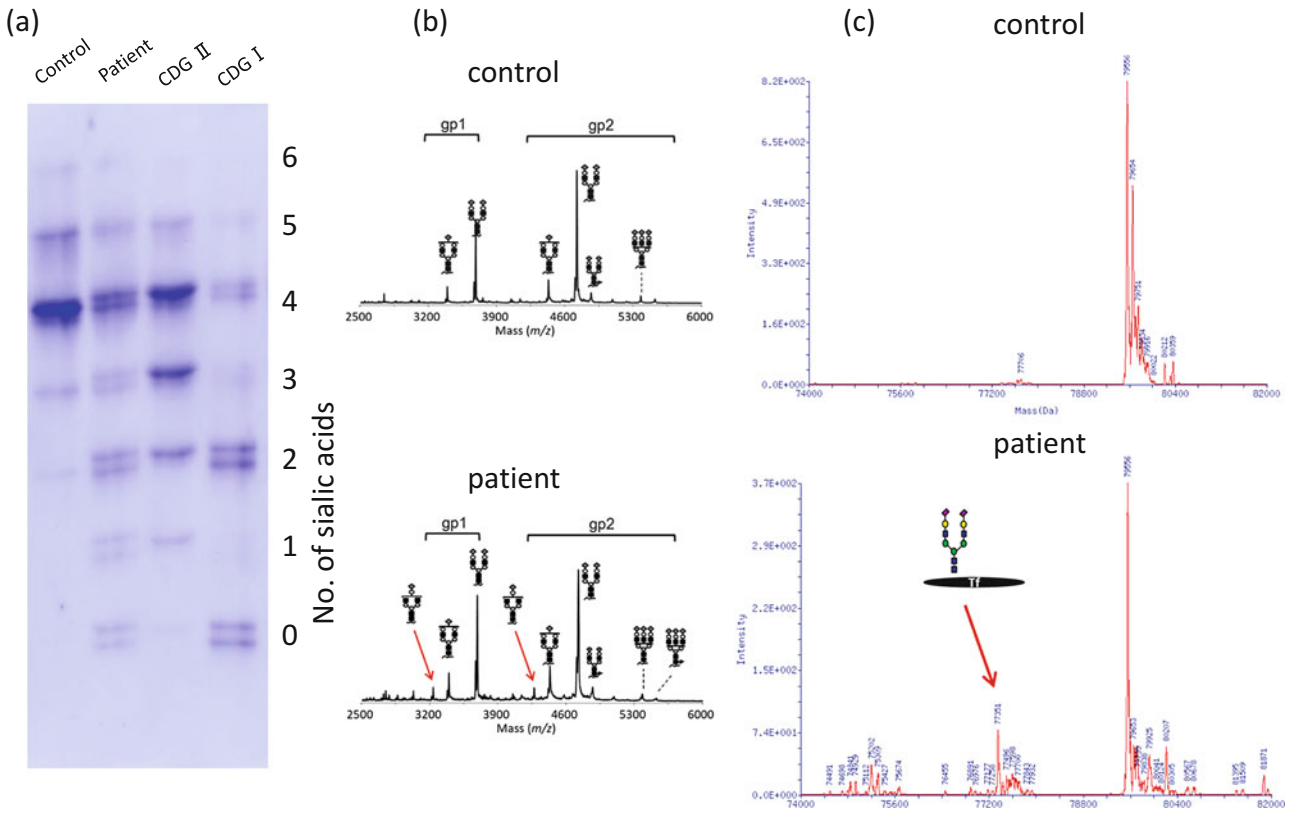

Fig. 2 Serum transferrin isoelectric focusing (IEF) and mass spectrometry (MS) of serum glycoproteins. (**a**) IEF patterns of serum transferrin. The number of negatively charged sialic acids of transferrin is indicated on the right. Reduced glycosylation of transferrin including an unusual mixture of CDG-I and CDG-II patterns (increased tri-, di-, mono-, and asialotransferrin) is shown. (**b**) Matrix-assisted laser desorption/ionization (MALDI) mass spectrum of (glycol) tryptic peptides of transferrin. A biantennary glycan lacking galactose and sialic acid are observed in patient's transferrin (arrows). (**c**) Electrospray ionization (ESI) mass spectrum of transferrin. An abnormal transferrin isoform having a single glycan is present in the patient (arrow)

genic mutations in the *PGM1* gene were identified and genetically confirmed in most of these cases (Perez et al. 2013; Ondruskova et al. 2014; Tagtmeyer et al. 2014; Loewenthal et al. 2015; Zeevaert et al. 2016; Wong et al. 2016; Preisler et al. 2017; Nolting et al. 2017; Voermans et al. 2017). However, a small subset of patients exists without mutations in the *PGM1* gene. In our present case, Sanger sequencing did not identify any pathogenic mutation in the *PGM1* gene initially. However, subsequent chromosome karyotyping of our patient detected the presence of multiple congenital malformations and led to the identification of the aforementioned chromosomal inversion as the responsible mutation for his condition. Hence, when standard molecular testing does not reveal any abnormalities in patients who have been clinically and biochemically diagnosed with a known congenital disorder, chromosome testing may be a fruitful approach for identifying the responsible mutation in the candidate gene.

In mutational screening for single-gene disorders involving an autosomal recessive inheritance of a known causative gene, it is often the case that only one of the recessive mutations is identified. If standard PCR and Sanger methods fail to identify two pathogenic mutations within the exons or flanking intronic regions of the responsible gene, a subsequent approach can be MLPA (multiplex ligation-dependent probe amplification) analysis of structural variant copy number variations or repeat PCR/Sanger analysis to identify possible mutations in noncoding regions such as the promoter or enhancer. In addition to these methods, standard chromosomal karyotyping is important for identifying large-scale chromosomal abnormalities that may disrupt the causative gene.

A possible mechanism of inversion formation is interspersed repeat sequences that may induce chromosomal aberrations. Direct repeats can induce deletions or duplications via recombination between them, whereas inverted repeats sometimes cause pericentric or paracentric inversion (Lakich et al. 1993). In our present case, we didn't find any specific segmental duplication sequences at the breakpoint region within the intron of the *PGM1* gene. Likewise, there was no evidence of segmental duplication sequences that were common to the proximal and distal breakpoint regions. Our patient harbored a rare homozygous pericentric inversion of chromosome 1 inherited from first-cousin parents. We assume

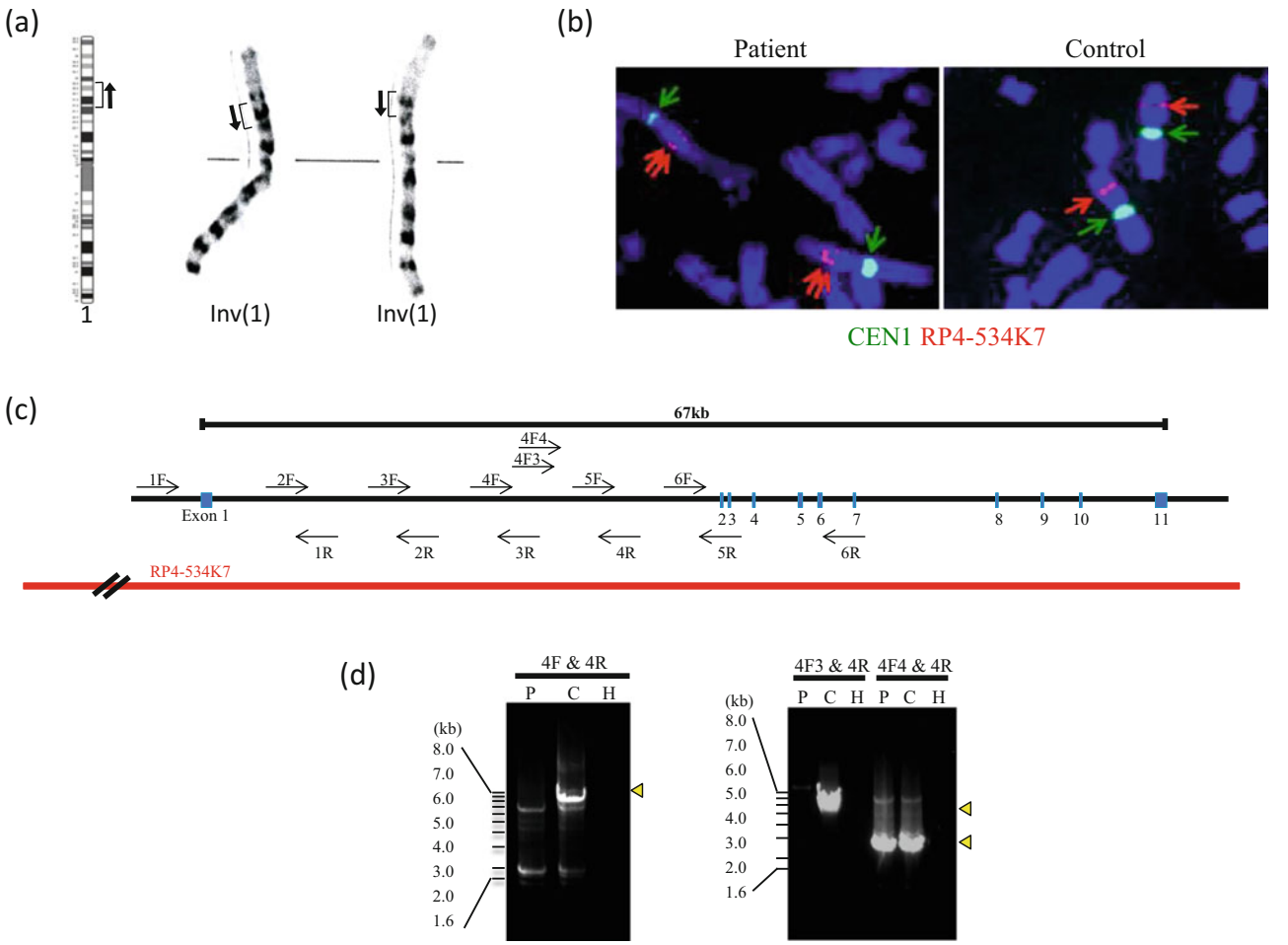

Fig. 3 Disruption of the *PGM1* gene in the study patient by a chromosomal inversion. (**a**) G-banding of the patient's karyotype which was determined to be 46,XY,inv(1)(p31.1p32.3)x2, in which inv(1) was homozygous. (**b**) FISH signals for *PGM1* (red arrow) are typically observed on the short arm of chromosome 1 in a normal karyotype. In contrast, the two distinctive signals were detected on the chromosome 1 arm in the study patient. (**c**) Schematic representation of the *PGM1* gene structure. The blue boxes denote exons. The positions of the PCR primers are indicated by arrows. The position of the BAC probe is also indicated. (**d**) Agarose gel electrophoresis of long PCR products. 4F-4R and 4F3-4R primer pairs failed to amplify the PCR products in the study patient. *P* patient, *C* control, *H* H_2O

therefore that the inversion chromosome in this patient is rare in the general population and is not a recurrent type variation.

Since the initiation codon in the *PGM1* gene is located within exon 1, the inversion in our patient that disrupts intron 1 produces a truncated protein containing only the amino acids encoded by exon 1 or no protein product at all due to nonsense-mediated mRNA decay. The crystal structure of human PGM1 has not been characterized, but the structure of the analogous PGM from rabbit has been described (Liu et al. 1997). Because of the high amino acid sequence identity (97%) between these two proteins, the rabbit PGM structure provides a highly accurate model for the human enzyme. PGM1 is a monomeric protein of 562 amino acids and 4 structural domains (Beamer 2015). The active site is located in a large, centrally located cleft and can be segregated into four highly conserved regions which are located behind exon 2. In our present case therefore, even if a truncated protein was produced, it would have no active site, and PGM1 deficiency would still arise. Further, we performed RT-PCR using the patient's peripheral blood. The exon 1 transcript was found to be present, but we did not find any transcripts distal to the exon 2 (data not shown). Some residual enzymatic activity might be possibly due to other members of phosphoglucomutase family, PGM2 and PGM3, that could compensate the PGM1 activity (Maliekal et al. 2007; Wong et al. 2016).

In conclusion, we have identified and analyzed an inverted chromosome from a PGM1 deficiency patient. Our present report also emphasizes the potential benefits of karyotype analysis in congenital cases in which molecular genetic testing fails to identify the responsible mutations.

Acknowledgments We thank the patient and his family for their participation in this study. We also thank past and present members of our laboratory. This research was partly supported by the intramural research grant (29-4) for Neurological and Psychiatric Disorders of NCNP (H. Sugie).

Synopsis Sentence

Karyotypic examination must be considered when standard molecular testing fails to reveal a mutation despite a positive clinical and biochemical diagnosis.

Conflict of Interest

Katsuyuki Yokoi, Yoko Nakajima, Ohye Tamae, Hidehito Inagaki, Yoshinao Wada, Tokiko Fukuda, Hideo Sugie, Isao Yuasa, Tetsuya Ito, and Hiroki Kurahashi declare that they have no conflict of interest.

Informed Consent

All procedures followed were in accordance with the ethical standards of the responsible committee on human experimentation (institutional and national) and with the Helsinki Declaration of 1975, as revised in 2005(5). Informed consent was obtained from all patients for inclusion in the study.

Author Contributions

Katsuyuki Yokoi retrieved the data and drafted and revised the manuscript.

Yoko Nakajima and Tetsuya Ito discovered the patients and provided many data.

Tamae Ohye did cytogenetic analysis and sequence analysis.

Hidehito Inagaki supported and supervised experiments.

Yoshinao Wada did mass spectrometry.

Tokiko Fukuda and Hideo Sugie estimated enzyme activity.

Isao Yuasa did IEF of serum transferrin.

Hiroki Kurahashi: conception and design, analysis and interpretation, and revising the article critically for important intellectual content.

All authors contributed to and reviewed the manuscript.

References

Beamer LJ (2015) Mutations in hereditary phosphoglucomutase 1 deficiency map to key regions of enzyme structure and function. J Inherit Metab Dis 38:243–256

Herbich J, Szilvassy J, Schnedl W (1985) Gene localisation of the PGM1 enzyme system and the Duffy blood groups on chromosome no. 1 by means of a new fragile site at 1p31. Hum Genet 70:178–180

Lakich D, Kazazian HH Jr, Antonarakis SE, Gitschier J (1993) Inversions disrupting the factor VII gene are a common cause of severe haemophilia A. Nat Genet 5:236–241

Lee Y, Stiers KM, Kain BN, Beamer LJ (2014) Compromised catalysis and potential folding defects in in vitro studies of missense mutants associated with hereditary phosphoglucomutase 1 deficiency. J Biol Chem 289:32010–32019

Liu Y, Ray W, Baranidharan S (1997) Structure of rabbit muscle phosphoglucomutase refined at 2.4A resolution. Acta Crystallogr D 53:392–405

Loewenthal N, Haim A, Parvari R, Hershkovitz E (2015) Phosphoglucomutase-1 deficiency: intrafamilial clinical variability and common secondary adrenal insufficiency. Am J Med Genet A 167A:3139–3143

Maliekal P, Sokolova T, Vertommen D, Veiga-da-Cunha M, Van Schaftingen E (2007) Molecular identification of mammalian phosphopentomutase and glucose-1,6-bisphosphate synthase, two members of the alpha-D-phosphohexomutase family. J Biol Chem 282:31844–31851

Morava E (2014) Galactose supplementation in phosphoglucomutase-1 deficiency; review and outlook for a novel treatable CDG. Mol Genet Metab 112:275–279

Nolting K, Park JH, Tegtmeyer LC et al (2017) Limitations of galactose therapy in phosphoglucomutase 1 deficiency. Mol Genet Metab Rep 13:33–40

Okanishi T, Saito Y, Yuasa I et al (2008) Cutis laxa with frontoparietal cortical malformation: a novel type of congenital disorder of glycosylation. Eur J Paediatr Neurol 12:262–265

Ondruskova N, Honzik T, Vondrackova A, Tesarova M, Zeman J, Hansikova H (2014) Glycogen storage disease-like phenotype with central nervous system involvement in a PGM1-CDG patient. Neuro Endocrinol Lett 35:137–141

Perez B, Medrano C, Ecay MJ et al (2013) A novel congenital disorder of glycosylation type without central nervous system involvement caused by mutations in the phosphoglucomutase 1 gene. J Inherit Metab Dis 36:535–542

Preisler N, Cohen J, Vissing CR et al (2017) Impaired glycogen breakdown and synthesis in phosphoglucomutase 1 deficiency. Mol Genet Metab 122:117–121

Scott K, Gadomski T, Kozicz T, Morava E (2014) Congenital disorders of glycosylation: new defects and still counting. J Inherit Metab Dis 37:609–617

Stojkovic T, Vissing J, Petit F et al (2009) Muscle glycogenosis due to phosphoglucomutase 1 deficiency. N Engl J Med 361:425–427

Tagtmeyer LC, Rust S, van Scherpenzeel M et al (2014) Multiple phenotypes in phosphoglucomutase 1 deficiency. N Engl J Med 370:533–542

Timal S, Hoischen A, Lehle L et al (2012) Gene identification in the congenital disorders of glycosylation type I by whole-exome sequencing. Hum Mol Genet 21:4151–4161

Voermans NC, Preisler N, Madsen KL et al (2017) PGM1 deficiency: substrate use during exercise and effect of treatment with galactose. Neuromuscul Disord 27:370–376

Wada Y (2016) Mass spectrometry of transferrin and apolipoprotein C-III for diagnosis and screening of congenital disorder of glycosylation. Glycoconj J 33:297–307

Wong SY, Beamer LJ, Gadomski T et al (2016) Defining the phenotype and assessing severity in phosphoglucomutase-1 deficiency. J Pediatr 175:130–136

Zeevaert R, Scalais E, Muino Mosquera L et al (2016) PGM1 deficiency diagnosed during an endocrine work-up of low IGF-1 mediated growth failure. Acta Clin Belg 71:435–437

Asian Journal of Andrology (2018) 20, 1–3
www.asiaandro.com; www.ajandrology.com

Open Access

LETTER TO THE EDITOR

Male Health

A constitutional jumping translocation involving the Y and acrocentric chromosomes

Makiko Tsutsumi[1], Naoko Fujita[1,2], Fumihiko Suzuki[3], Takashi Mishima[4], Satoko Fujieda[4], Michiko Watari[4], Nobuhiro Takahashi[5], Hidefumi Tonoki[5], Osamu Moriwaka[6], Toshiaki Endo[7], Hiroki Kurahashi[1,2,3]

Asian Journal of Andrology (2018) **20**, 1–3; doi: 10.4103/aja.aja_60_18; published online: ???

Dear Editor,

Translocations of the same chromosomal fragments to two or more different chromosomes in different somatic cell lineages are referred to as jumping translocations (JTs).[1] JTs have been mainly reported in hematological malignancies but have been observed in rare instances also as constitutional chromosomal aberrations.[2] The underlying JT mechanism remains unclear, however.

The frequency of Y-autosome translocations is 1 in 2000 and carriers are often identified through spermatogenic defects or by an incidental finding in the absence of clinical symptoms.[3] Notably, translocations of the heterochromatin region of the Y long arm to the short arm of chromosome 15 or 22 are commonly observed as normal variants.[4] We here present an intriguing case of a constitutional Y;13 translocation in a male with oligozoospermia but a Y;15 translocation in his son, who was born with the assistance of reproductive technologies. To uncover the origin of this inconsistency, we examined the Y-autosome translocated chromosomes and concluded that this represented an instance of JT.

Our study family included a 40-year-old male partner of a Japanese infertile couple who was healthy except for a severe oligozoospermia identified during a prior examination for causes of the couple's infertility. As detailed below, he was found to carry a Y;13 translocation. The female partner was 38-year-old with a 46,XX karyotype. This couple had three prior miscarriages before becoming pregnant via intracytoplasmic sperm injection, which produced a healthy boy with normal external genitalia. The genetic testing used in our current analyses was approved by the ethics committee of Fujita Health University (Toyoake, Japan). Blood samples from the participants were obtained following written informed consent in accordance with Local Institutional Review Board guidelines.

G-banding analysis of the father revealed a 45,X,add(13)(p11) karyotype (**Figure 1a**). Fluorescent *in situ* hybridization (FISH) analyses with Y chromosome probes were conducted to determine the origin of the additional chromosomal material. A Yp telomere probe produced a positive signal at the add(13) chromosome (**Figure 2a**). *SRY* (sex-determining region Y), DYZ3 (alphoid satellite DNA) and *DAZ* (deleted in azoospermia) probes were also positive at add(13) (data not shown). No signal for DYZ1, a Y-specific heterochromatin repeat (Yqh), was evident on add(13) or on other chromosomes (data not shown). These results indicated that the additional chromosome in the father was a Y chromosome lacking the distal part of the long arm that had fused with the short arm of chromosome 13 (**Figure 1c** and **2a**). The breakpoint on the Y chromosome was located in the proximity of the boundary region between *DAZ* and the heterochromatin region, and that on chromosome 13 was located in its short arm (**Figure 1c**). Thus, the add(13) chromosome was dicentric, lacking the 13p region. Consequently, the father's karyotype was 45,X,add(13)(p11).ish dic(Y;13)(q11.2 or q12;p11)(SRY+,DYZ3+,DAZ+).

Interestingly, both an amniocentesis and analysis of peripheral blood from the son obtained after birth indicated a karyotype of 45,X,add(15)(p11.2).ish psu dic(15;Y)(p11.2;q11.2)(SRY+,DYZ3+,DAZ+) (**Figure 1b** and **2b–2d**). Unlike father, the Y chromosome material of the son was joined to chromosome 15 and not chromosome 13 (**Figure 1c**).

The haplotypes of the Y chromosomal regions in both the father and son were analyzed by evaluating common STR markers using the AmpFLSTR Yfiler PCR Amplification Kit (Thermo Fisher Scientific, Waltham, MA, USA). The amplification of 17 Y-chromosomal STR loci in both father and son indicated a perfect match (**Table 1**). Furthermore, as the frequency of this haplotype would be expected to be approximately 1 in 6135 in Japan, as calculated using the Kappa method (release R54; https://yhrd.org),[5,6] this finding was very unlikely to have been coincidental. Our analysis thus indicated that the son inherited his Y chromosomal material from his father and that a second translocation event involving the Y chromosomal region occurred during paternal spermatogenesis.

We therefore here report a rare event in which a translocated Y chromosome changed partner chromosomes during its transmission to the next generation. We refer to this as JT. To the best of our knowledge, only one other family has been previously described in which a constitutional JT involving the Y chromosome occurred between a father, tas(Y;19), and son, tas(Y;15).[7] Telomeric associations (TAS) refer to a fusion between telomeres of different chromosomes. As defective

[1]Division of Molecular Genetics, Institute for Comprehensive Medical Science, Fujita Health University, Toyoake 470-1192, Japan; [2]Genome and Transcriptome Analysis Center, Fujita Health University, Toyoake 470-1192, Japan; [3]Center for Collaboration in Research and Education, Fujita Health University, Toyoake 470-1192, Japan; [4]Department of Obstetrics and Gynecology, Tenshi Hospital, Sapporo 065-8611, Japan; [5]Department of Pediatrics, Tenshi Hospital, Sapporo 065-8611, Japan; [6]Kamiya Ladies Clinic, Sapporo 060-0003, Japan; [7]Department of Obstetrics and Gynecology, Sapporo Medical University, Sapporo 060-8556, Japan.
Correspondence: Dr H Kurahashi (kura@fujita-hu.ac.jp)
Received: 18 January 2018; Accepted: 20 June 2018

Table 1: Haplotypes of the Y-STR loci in the father and son

	DYS456	*DYS389I*	*DYS390*	*DYS389II*	*DYS458*	*DYS19*	*DYS385*	*DYS393*	*DYS391*	*DYS439*	*DYS635*	*DYS392*	*YGATAH4*	*DYS437*	*DYS438*	*DYS448*
Father	16	14	23	29	18	16	10, 19	14	10	11	20	13	12	14	13	18
Son	16	14	23	29	18	16	10, 19	14	10	11	20	13	12	14	13	18

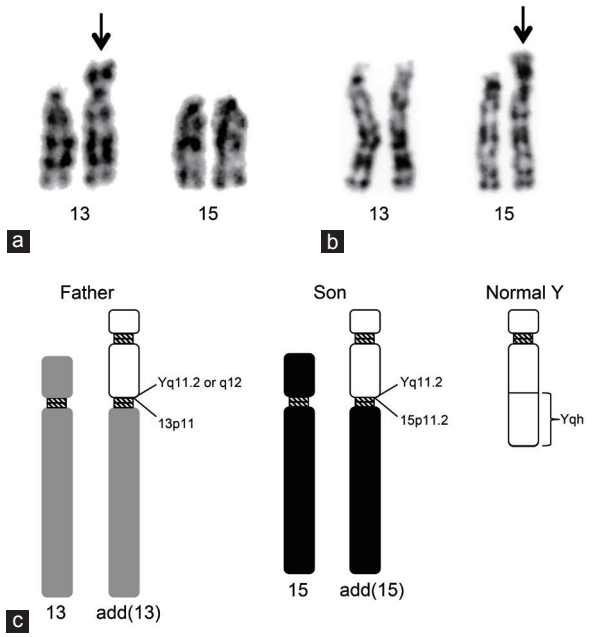

Figure 1: G-banded partial karyotypes of the father and son. (**a**) The arrow denotes the add(13) in the father. (**b**) The arrow indicates the add(15) in the son. (**c**) Schematic diagram of the translocated chromosomes. The breakpoints of each translocation are indicated. The Yqh regions are lost in both the father and son.

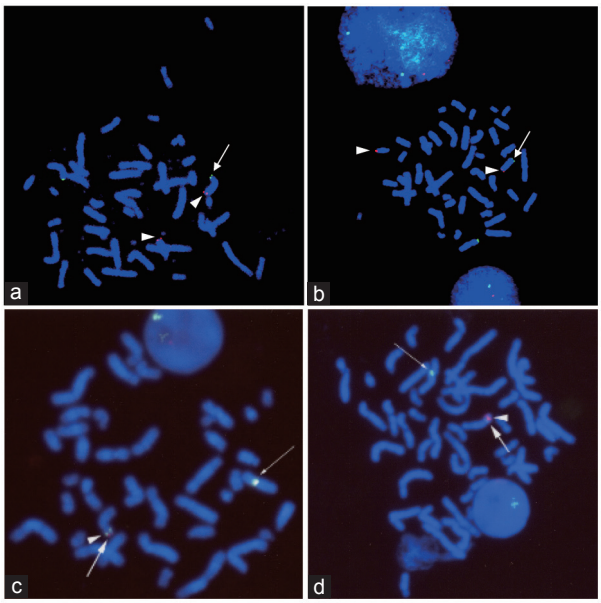

Figure 2: FISH analyses of the translocated chromosomes in the father and son. (**a**) Xp/Yp telomere (green) and 13q telomeres (red) in the father. The arrow and arrowheads denote the Yp and 13q probes, respectively. (**b**) Xp/Yp telomere (green) and 15q telomeres (red) in the son. The arrow and the arrowheads indicate the Yp and 15q probes, respectively. (**c**) *SRY* (red, large arrow), DYZ3 (green, arrowhead) and DXZ1 (green, small arrow) in the son. (**d**) *DAZ* (green, large arrow), DYZ3 (red, arrowhead) and DXZ1 (green, small arrow) in the son. Chromosomes were counterstained with DAPI (blue).

telomeric repeats at the junction can elicit conformational instability, it is quite possible that one TAS event could induce another and thereby lead to JT. Our present case was not the result of a TAS event however because the Yqter was lacking at the junction, although it is possible that the junction of the first translocation was unstable due to an unknown sequence-specific mechanism leading to a susceptibility for a second translocation.

Like most constitutional JTs thus far described, our present case family involved acrocentric chromosomes in both translocations.[2] JT breakpoints mostly reside in centromeric/pericentromeric regions or within telomeric sequences, which involve heterochromatin and are rich in repetitive DNA.[8] Chromosome breakages associated with JTs frequently occur at repetitive DNA regions because of their genomic instability.[9] In our current subject family, it is likely that the dic(Y;13) junction comprising a fusion of repetitive DNA of both chromosomal regions produced increased instability as a result of the first translocation. It has been shown that the short arms of the acrocentric bivalents associate with the nucleoli during prophase of meiosis I.[10] The dic (Y;13) paired with the normal chromosome 13 should, therefore, be involved in the nucleolus and come close to the short arm of the bivalent chromosome 15. It is possible that this proximity and the unstable junction might have induced the second translocation in a spermatocyte.

In conclusion, a rare JT event occurred during spermatogenesis in a Japanese man with oligozoospermia and was transmitted to his son. Although it is rare, a JT should be considered in cases where there is an inconsistency between the translocated chromosomes in a parent and child.

AUTHOR CONTRIBUTIONS

MT carried out the cytogenetic analysis, STR analysis and drafting of the manuscript. NF and FS performed the cytogenetic analysis. TM and SF carried out the gynecological check and provided genetic counseling. MW provided the genetic counseling for the prenatal test. NT carried out the clinical management of the son. HT was responsible for the chromosomal analysis and the clinical genetics. OM conducted the fertility treatment. TE and HK conceived the study and participated in its design. HK drafted the manuscript. All authors read and approved the final manuscript and agreed with the order of presentation of the authors.

COMPETING INTERESTS

The authors declare no competing interests.

ACKNOWLEDGMENTS

This study was supported by a grant-in-aid for Scientific Research from the Ministry of Education, Culture, Sports, Science, and Technology of Japan, that from the Ministry of Health, Welfare and Labor, and that from Japan Agency for Medical Research and Development.

REFERENCES

1 Lejeune J, Maunoury C, Prieur M, Van den Akker J. A jumping translocation (5p;15q), (8q;15q), and (12q;15q). *Ann Genet* 1979; 22: 210–3.
2 Reddy KS. The conundrum of a jumping translocation (JT) in CVS from twins and review of JTs. *Am J Med Genet A* 2010; 152A: 2924–36.

3 Alves C, Carvalho F, Cremades N, Sousa M, Barros A. Unique (Y;13) translocation in a male with oligozoospermia: cytogenetic and molecular studies. *Eur J Hum Genet* 2002; 10: 467–74.
4 Gardner RJ, Sutherland GR, Shaffer LG. Chromosome Abnormalities and Genetic Counseling. 4th ed. New York, Oxford: Oxford University Press; 2011. p 98-121.
5 Willuweit S, Roewer L. The new Y chromosome haplotype reference database. *Forensic Sci Int Genet* 2015; 15: 43–8.
6 Brenner CH. Fundamental problem of forensic mathematics – The evidential value of a rare haplotype. *Forensic Sci Int Genet* 2010; 4: 281–91.
7 Huang B, Martin CL, Sandlin CJ, Wang S, Ledbetter DH. Mitotic and meiotic instability of a telomere association involving the Y chromosome. *Am J Med Genet A* 2004; 129A: 120–3.
8 Berger R, Bernard OA. Jumping translocations. *Genes Chromosomes Cancer* 2007; 46: 717–23.
9 Reddy KS, Murphy T. Fusion of 9 beta-satellite and telomere (TTAGGG)n sequences results in a jumping translocation. *Hum Genet* 2000; 107: 268–75.
10 Stahl A, Luciani JM, Hartung M, Devictor M, Bergé-Lefranc JL, *et al*. Structural basis for Robertsonian translocations in man: association of ribosomal genes in the nucleolar fibrillar center in meiotic spermatocytes and oocytes. *Proc Natl Acad Sci U S A* 1983; 80: 5946–50.

JOURNAL OF OBSTETRICS AND GYNAECOLOGY, 2018
https://doi.org/10.1080/01443615.2017.1401598

Taylor & Francis
Taylor & Francis Group

CASE REPORT

Twin pregnancy with chromosomal abnormalities mimicking a gestational trophoblastic disorder and coexistent foetus on ultrasound

Akiko Ohwaki[a,b], Haruki Nishizawa[a], Noriko Aida[a], Takema Kato[b], Asuka Kambayashi[a], Jun Miyazaki[a,b], Mayuko Ito[a,b], Makoto Urano[c], Yuka Kiriyama[c], Makoto Kuroda[c], Masahiro Nakayama[d], Shin-Ichi Sonta[e], Kaoru Suzumori[e], Takao Sekiya[a], Hiroki Kurahashi[b] and Takuma Fujii[a]

[a]Department of Obstetrics and Gynecology, Fujita Health University School of Medicine, Toyoake, Japan; [b]Division of Molecular Genetics, Institute for Comprehensive Medical Science, Fujita Health University, Toyoake, Japan; [c]Department of Diagnostic Pathology, Fujita Health University School of Medicine, Toyoake, Japan; [d]Department of Pathology and Laboratory Medicine, Osaka Medical Center and Research Institute for Maternal and Child Health, Izumi, Japan; [e]Fetal Life Science Center, Ltd, Nagoya, Japan

Case report

Gestational trophoblastic disorder with a coexistent foetus occurs in 1 in 20,000–100,000 pregnancies (Wee and Jauniaux 2005) and mostly involves a partial hydatidiform mole with a live foetus and rarely a twin pregnancy with a complete hydatidiform mole and co-twin foetus (Gupta et al. 2015). Most cases of partial hydatidiform mole have triploidy with multiple structural anomalies and result in first trimester miscarriage (Toufaily et al. 2016). However, their management is complicated because the coexistent foetus is occasionally a normal healthy diploid foetus. Furthermore, this condition is often accompanied by severe complications such as hyperemesis, preeclampsia or thromboembolic disease (Matsui et al. 2000; Sebire et al. 2002). Thus, the diagnosis and management of gestational trophoblastic diseases with coexistent foetus are clinically important.

A gravid 33-year-old woman (gravid 4, para 3) was referred to our hospital with vaginal bleeding from 9 weeks of gestation. She was noted on prenatal ultrasound to have a normal foetus with an abnormally thickened space in the placental region. At 11 gestational weeks, a snowstorm pattern was observed on ultrasound examination, but it was slightly different from the typical pattern for hydatidiform mole. Multivesicular areas were prominent, but the other areas appeared relatively normal (Figure 1(A)). At 13 gestational weeks, the snowstorm pattern persisted with a foetal growth retardation of a biparietal diameter of 22.3 mm (−1.9 SD). The serum β-human chorionic gonadotropin (β-hCG) level was alarmingly elevated at 369,065 mIU/ml at 14 gestational weeks, whereas alpha-fetoprotein (AFP) showed a normal level of 109.5 ng/ml. β-hCG was persistently high at 207,336 mIU/ml at 16 gestational weeks, whereas AFP was 159.8 ng/ml.

The couple decided to terminate the pregnancy after considering the risks because the possibility of hydatidiform mole and coexistent foetus could not be excluded. After the curettage, the woman was in good condition and the β-hCG level decreased to 4 mIU/ml. The delivered foetus had a median cleft lip and palate (Figure 1(B)). The placenta appeared to have patchy villous hydropic changes (Figure 1(C)). Histological examination revealed focal villous oedema. Trophoblast hyperplasia was not observed (Figure 1(D)). After receiving approval from the Ethical Review Board and obtaining written informed consent from the couple, we obtained samples from the foetal skin and from the oedematous and normal-seeming areas of the placenta.

Initial cytogenetic analysis by Giemsa staining indicated a normal karyotype (data not shown). Cytogenetic microarray of the foetus revealed three copies of an 8-Mb region at the terminus of 9p, but monosomy 2q and trisomy 4q in the placenta (Figure 1(E–G)). Although hydatidiform moles generally result from dispermic triploidy or diandric diploidy with the paternal genome only, there was no evidence of triploidy or uniparental disomy. The foetus was found to carry arr[hg19] 9p24.3p24.1(326,927–8,441,863)x3, which appeared to be mosaic with normal cells because the copy number (CN) state was 2.80. On the other hand, the placental tissue was found to carry arr[hg19] 2q37.3(237,337,625–242,408,074)x1, 4q25q35.2(113,816,349–190,957,.473)x3. These appeared to be in mosaicism because the CN state was 1.35 and 2.67, respectively. Approximately 65–67% of cells showed monosomy 2q and trisomy 4q, and it is likely that the same cells had monosomy 2q and trisomy 4q simultaneously. The placental tissue also showed 9p trisomy at CN state 2.33, suggesting that 33% of cells carried the 9p trisomy identified in the foetus. On the other hand, we did not detect monosomy 2q and trisomy 4q in foetal tissue at all.

Microsatellite analysis of the DXS0767 locus revealed that there was only a small level of maternal tissue contamination in placental tissue (2–3%, data not shown) and none in foetal tissue. The pattern of whole-genome SNP genotyping also excluded the chimeric pattern but indicated a single zygote origin, suggesting that all of the foetus and placenta were derived from a monozygotic twin or somatic

CONTACT Haruki Nishizawa nharuki@fujita-hu.ac.jp Department of Obstetrics and Gynecology, Fujita Health University, 1-98 Dengakugakubo, Kutsukake, Toyoake, Aichi, 470-1192 Japan

Supplemental data for this article can be accessed here.

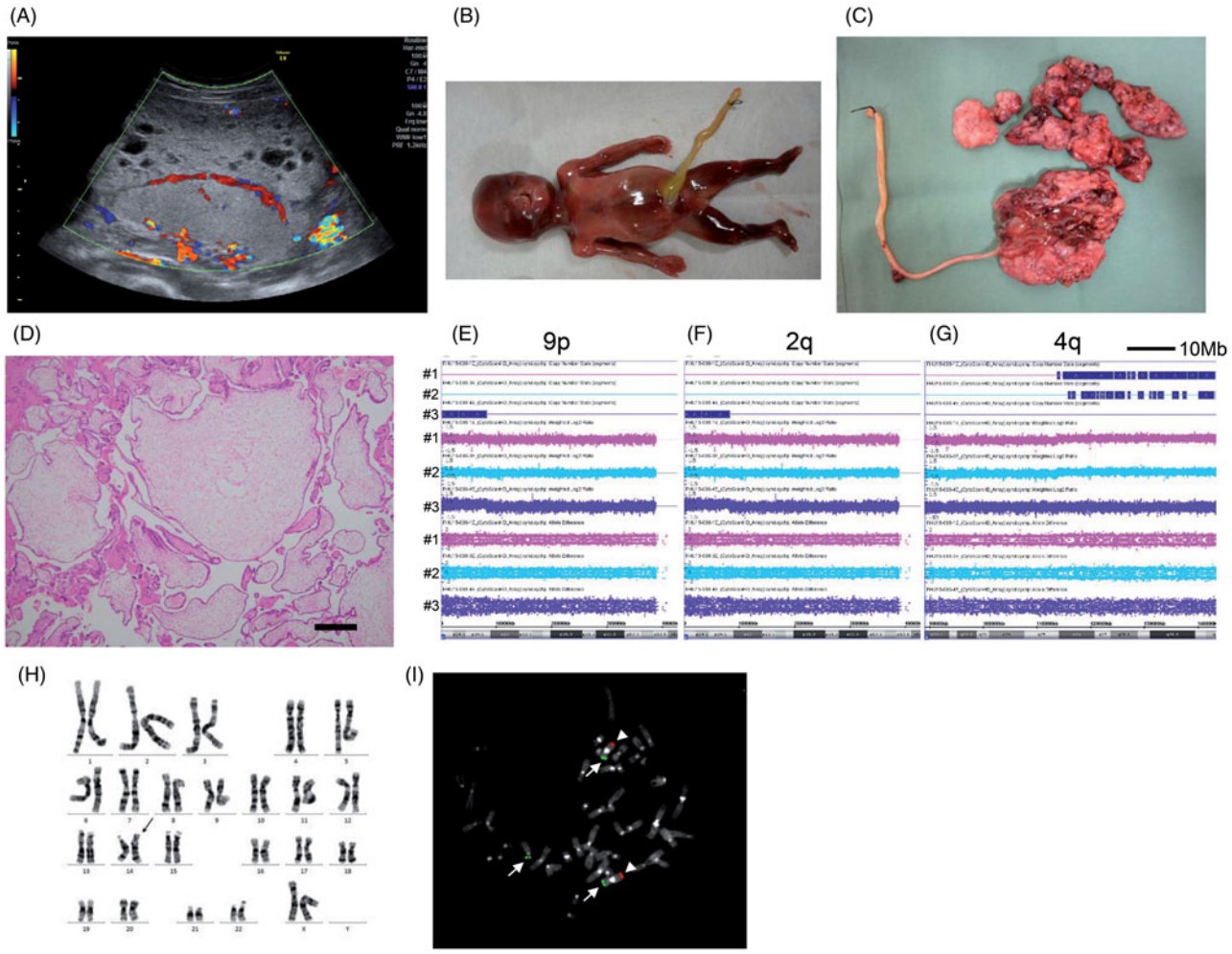

Figure 1. Clinical phenotypes and cytogenetic analysis of the foetus and placenta. Cytogenetic microarray was performed using CytoScan HD Array (Affymetrix). #1: placenta that appeared relatively normal; #2: placenta that included villous hydrops lesions; and #3: foetus. (A) Ultrasound examination at 11 weeks of gestation. Two separate areas – a vesicular area (upper area) and relatively normal area (lower area) – were observed, which are atypical for gestational trophoblastic disease. (B) Foetus. A median cleft lip and palate were observed. (C) Macroscopic analysis of the placenta. Patchy villous hydropic changes were observed. (D) Histological specimen for chorionic villi. Focal villous oedema was observed. Scale bars, 100 m. (E) 9p and 9q. (F), 2q. (G), 4q. Scale bars, 10 Mb. (H), Giemsa staining. Additional material was observed at the terminal region of 14p. (I) FISH. Subtelomeric probes (Vysis ToTelVision, Abbott Molecular) revealed the presence of der(14)t(9;14)(p24;p11.2) (arrow). White arrows: 9p; and white arrow heads: 9q.

mosaicism of a single zygote. As the CN state showed that the cell population with 9p and that with monosomy 2q and trisomy 4q were mutually exclusive, we concluded that they were likely from monozygotic twins (Supplementary Figure).

Reexamination of Giemsa staining of the foetal fibroblasts showed additional material at the terminal of 14p. Subtelomeric FISH was performed to further characterise the CN abnormalities. Trisomy 9p was found to originate from der(14)t(9;14)(p24; p11.2) in all of the 20 metaphases examined (Figure 1(H,I)). As the CN states of monosomy 2q and trisomy 4q are reciprocal, the monosomy 2q and trisomy 4q found in the placenta were likely to have originated from unbalanced t(2;4)(q37.3; q25) translocation. However, subtelomeric FISH did not detect the t(2;4) translocation in any of the foetal cells. We did not study the karyotype of the couple because they did not want to undergo the required examinations.

We recommend careful performance of the differential diagnosis of abnormal placenta with snowstorm pattern, particularly in cases with a coexistent foetus. A molecular cytogenetic study including zygosity test is necessary for differential diagnosis because it is possible that a chromosomal disorder might underlie placental abnormalities. The severities of the clinical symptoms in the foetus with such disorders vary widely. These disorders often result in lethality from multiple congenital anomalies, whereas cases with milder cytogenetic abnormalities can occasionally survive and live to a good age. Furthermore, confined placental mosaicism might affect the foetus to a lesser degree (Johnson and Wapner 1997; Lestou and Kalousek 1998). Thus, the results of the cytogenetic test might seriously affect the choice of treatment for the ultrasound findings.

Acknowledgements

We gratefully acknowledge the patients and their families for participating in this study.

Disclosure statement

The authors report no conflicts of interest.

Funding

This study was supported by the Ogyaa Donation Foundation from the Japan Association of Obstetricians & Gynecologists and by grants-in-aid for Scientific Research from the Ministry of Education, Culture, Sports, Science, and Technology and from the Ministry of Health, Labour and Welfare of Japan.

References

Gupta K, Venkatesan B, Kumaresan M, Chandra T. 2015. Early detection by ultrasound of partial hydatidiform mole with a coexistent live fetus. WMJ: Official Publication of the State Medical Society of Wisconsin 114:208–211.

Johnson A, Wapner RJ. 1997. Mosaicism: implications for postnatal outcome. Current Opinion in Obstetrics & Gynecology 9:126–135.

Lestou VS, Kalousek DK. 1998. Confined placental mosaicism and intrauterine fetal growth. archives of disease in childhood. Fetal and Neonatal Edition 79:F223–F226.

Matsui H, Sekiya S, Hando T, Wake N, Tomoda Y. 2000. Hydatidiform mole coexistent with a twin live fetus: a national collaborative study in Japan. Human Reproduction (Oxford, England) 15:608–611.

Sebire NJ, Foskett M, Paradinas FJ, Fisher RA, Francis RJ, Short D, et al. 2002. Outcome of twin pregnancies with complete hydatidiform mole and healthy co-twin. Lancet (London, England) 359:2165–2166.

Toufaily MH, Roberts DJ, Westgate MN, Holmes LB. 2016. Triploidy: variation of phenotype. American Journal of Clinical Pathology 145:86–95.

Wee L, Jauniaux E. 2005. Prenatal diagnosis and management of twin pregnancies complicated by a co-existing molar pregnancy. Prenatal Diagnosis 25:772–776.